Available online at www.sciencedirect.com
SCIENCE DIRECT®
Coordination Chemistry Reviews 246 (2003) 103–130
COORDINATION CHEMISTRY REVIEWS
www.elsevier.com/locate/ccr

Structure and magnetism of coordination polymers containing dicyanamide and tricyanomethanide

Stuart R. Batten*, Keith S. Murray*

Department of Chemistry, School of Chemistry, Monash University, Clayton, Vic. 3800, Australia

Received 12 March 2003; accepted 17 June 2003

Contents

Abstract

Coordination polymers containing dicyanamide ($N(CN)_2^-$, dca) or tricyanomethanide ($C(CN)_3^-$, tcm) bridging ligands are described from the perspective of their structure and magnetism. The binary compounds α-$M(dca)_2$ form an isostructural series (M = Cr, Mn, Fe, Co, Ni, Cu) having a single rutile-like network that involves $\mu_{1,3,5}$-dca bridging. They display quite diverse types of long-range magnetic order viz. canted-spin antiferromagnets (Cr, Mn, Fe), ferromagnets (Co, Ni, Cu). An up-to-date review is given of the diverse range of physical measurements made on the α-$M(dca)_2$ series together with interpretations for the different net exchange coupling and consequent 3D order. The doubly interpenetrating rutile network $M(tcm)_2$ series generally do not show long-range order except for a few members at very low temperatures. The 'mixed' self-penetrating network compounds M(dca)(tcm) do show long-range order (M = Co, Ni), albeit at lower T_c values than for the $M(dca)_2$ parents. Modification of the M–dca networks is possible by incorporation of coligands into the structures. Ternary species of type $M(dca)_2(L)_n$, where L is a terminal (e.g. pyridine, MeOH) or a bridging (e.g. pyrazine, 4,4′-bipyridine) coligand, display a diverse range of 1D, 2D and 3D structural types. With a few exceptions, the large number of compounds structurally characterised contain $\mu_{1,5}$-dca bridging and display very weak antiferromagnetic coupling ($J <$ ca. -1 cm^{-1}), typical of this bridging mode. Compounds such as $Mn(dca)_2$(pyrazine) display a magnetic phase transition at low temperatures. This is also the case in the isostructural 2D layer compounds $M(dca)_2(H_2O)\cdot$phenazine (M = Fe, Ni) which, perhaps not surprisingly, do not have coordinated phenazines but, rather, phenazines intercalated between layers of $M(dca)_2(H_2O)$ in which $\mu_{1,3,5}$ and $\mu_{1,5}$-dca bridging exists. Anionic networks of types $M(dca)_3^-$ and $M(dca)_4^{2-}$ formed by templation around cations of the organic (e.g. Ph_4E^+, R_4N^+) or inorganic ($M(2,2'\text{-bipyridine})_3^{2+}$) types are described.

* Corresponding authors. Fax: +61-3-9905-4597.
E-mail addresses: stuart.batten@sci.monash.edu.au (S.R. Batten), keith.s.murray@sci.monash.edu.au (K.S. Murray).

doi:10.1016/S0010-8545(03)00119-X

The latter display no magnetic interactions between the weakly antiferromagnetically coupled anionic sub-lattice and the paramagnetic cationic sub-lattice.

Keywords: Coordination polymers; Crystal engineering; Dicyanamide; Tricyanomethanide; Molecule-based magnetism

1. Introduction

The modular, topological approach to both the design and description of coordination polymers, espoused by Robson and Hoskins in their seminal 1990 paper [1], has blossomed in the last 6 or 7 years to become a very wide field of research [2,3]. Applications [4] of such crystal engineering include microporous materials (including use in gas storage) [5], heterogeneous catalysis [6], non-linear optical activity [7], molecular sensors [8], magnetic switches [9] and molecule-based magnets [10,11].

The coordination polymers of pseudohalide ligands such as cyanide, azide and thiocyanate have long been studied for their interesting magnetic properties [12,13]. Of late, however, the larger pseudohalide ligands dicyanamide (dca, $N(CN)_2^-$) and tricyanomethanide (tcm, $C(CN)_3^-$) have been attracting a lot of attention, partly due to the discovery of long-range magnetic ordering in the α-$M(dca)_2$ compounds [14–16]. Therefore, it is timely to review this area of chemistry.

This review will focus mainly on compounds that have been crystallographically characterised, are polymeric, and have bridging dca or tcm ligands. Structures with only monodentate [17,18] and uncoordinated [17r,17s,19] dca and tcm ligands will largely be ignored, as will those molecular structures containing bridging dca or tcm ligands [18,20]. A particular focus will be the magnetic properties of these polymeric materials. For further details, especially for non-crystallographically characterised systems, the reader is directed to a number of other reviews on these compounds [21–25]. A considerable amount of earlier work, particularly by Köhler et al., is also eminently noteworthy. Many of the compounds now being re-examined with the benefit of modern crystallographic and magnetic instrumentation were first synthesised in the period between the mid-1960s and the early 1980s by Köhler and co-workers [21].

A particular feature of the dca and tcm ligands is the variability in coordination modes they can display (Schemes 1 and 2). To this end, we will use a system of notation throughout this review to describe succinctly the binding modes encountered. This will take the form $\mu_{a,b,c,\ldots}$, where the subscripts denote the nitrogen atoms which are coordinating to metal ions. For dca these can have the values 1, 3 or 5, while for tcm the possible values are 1, 5 or 7. The amide nitrogen in dca is assigned the index 3, and the notation μ_3-dca indicates a monodentate dca binding through the amide nitrogen atom, and not a tridentate dca anion. For tcm, unless otherwise stated, bidentate and tridentate refer to coordination via two and three nitrile nitrogen atoms only (i.e. $\mu_{1,5}$ and $\mu_{1,5,7}$, respectively). When a particular nitrogen atom coordinates to more than one metal ion, the number representing that atom is repeated as many times as required. Binding modes reported to date are shown in Schemes 1 and 2.

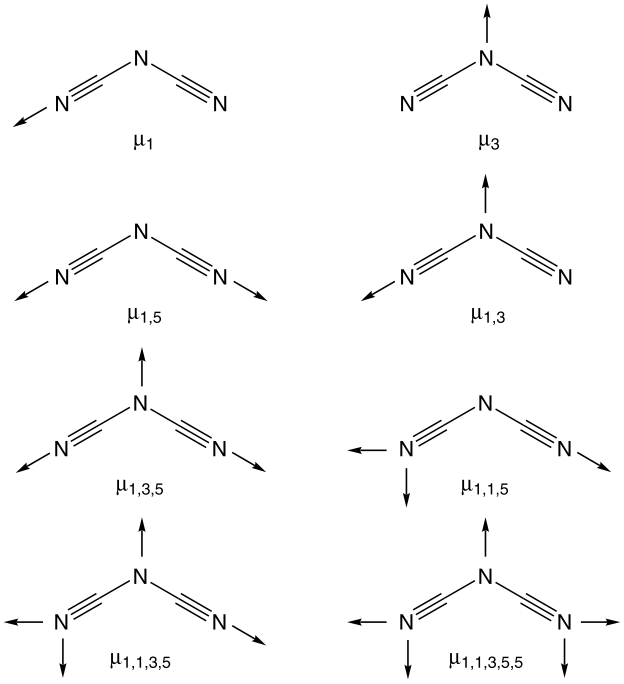

Scheme 1. Dca coordination modes observed to date.

The magnetic exchange coupling constants, *J*, quoted in the following sections are based on the spin Hamiltonian

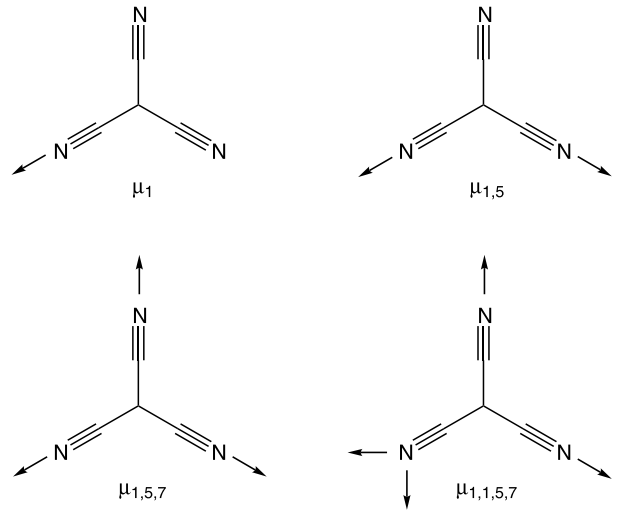

Scheme 2. Tcm coordination modes observed to date.

$-J\mathbf{S_1} \cdot \mathbf{S_2}$, used in the various 1D, 2D and 3D models. Values of J are usually given in cm^{-1} but occasionally, as J/k_B, in temperature units K ($k_B = 0.699\ cm^{-1}\ K^{-1}$).

2. Binary M(dca)$_2$ and related compounds

2.1. Magnetic systems

Observation of long-range magnetic order in the binary d-block dicyanamide series of complexes α-M(dca)$_2$ [14–16], caused great interest, excitement and competition, not only because these were homometallic species, but because they provided new examples of molecular network materials which enhanced the knowledge gained in the 1980–1990s on heterometallic μ-oxalato [10,11], μ-oxamido [10] and μ-cyano (Prussian blue) [10,12] molecular magnets.

The structures of the isomorphous series α-M(dca)$_2$, M = Cr, Mn, Fe, Co, Ni, Cu contain 3D networks (Fig. 1) of octahedral metal ions bridged by $\mu_{1,3,5}$-dca ligands [14–16,26,27]. The networks have the same topology as that of rutile (TiO_2), with six-connecting centres (metal atoms) and three-connecting centres (dca ligands) in the ratio of 1:2. The metal ions are coordinated to four-equatorial dca ligands via their nitrile nitrogens and to two-axial dca ligands via their amide nitrogens; in the Cu salt considerable Jahn–Teller elongation (by ca. 0.5 Å) of the axial Cu–N(amide) bonds is observed. The M–N(amide) bonds are also longer than the M–N(nitrile) interactions in all the other crystallographically characterised members of this series, although the difference is only ca. 0.1 Å or less.

As mentioned above and in Section 1, these compounds show long-range magnetic ordering, and their magnetic and other properties have been extensively studied recently using a wide variety of techniques ranging from DC magnetic susceptibilities and magnetisation (in field-cooled (FCM), zero-field cooled (ZFCM) and remnant magnetisation (RM) modes), AC magnetic susceptibilities, specific heat, neutron diffraction [28,29], muon spin relaxation [30,31] and Mössbauer spectroscopy (α-Fe(dca)$_2$) [32,33]. Ambient pressure and high pressure studies have been made using some of these techniques [34].

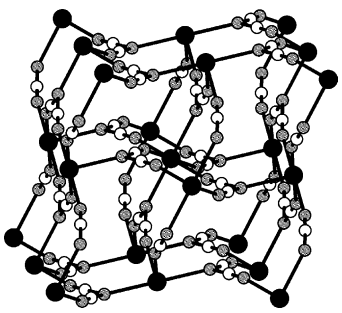

Fig. 1. The rutile-like 3D structure of α-M(dca)$_2$. Metal atoms are shown in black, nitrogen atoms in grey, carbon in white.

The types of magnetic order and the key magnetic parameters are given in Table 1. Detailed discussions of these parameters, such as the large coercive field in the hard molecular magnets α-Fe(dca)$_2$ and α-Ni(dca)$_2$, and factors which affect the coercive field, have been given [15]. The detailed physics of the magnetic structures has been probed by Epstein et al. using neutron powder diffraction studies [28,29]. α-Mn(dca)$_2$ has a non-collinear antiferromagnetic structure [29] in which two sublattices are antiferromagnetically coupled and canted with respect to each other. The spin-orientation is mainly along the *a*-axis with a small uncompensated component along *b*. The spin-canting is induced by the successive tilting of the MnN_6 octahedra in combination with magnetic anisotropy on the Mn(II) $^6A_{1g}$ centres in the *ab* plane. The canting angle has been estimated to give quite diverse values [29], but 0.05° is now accepted [27]. Lappas et al. [35] have also recently studied the powder neutron diffraction of α-Mn(dca)$_2$. While broadly agreeing with Epstein et al. [29] that the antiparallel component of the two sublattices is along *a* and the parallel component along *b*, they note that symmetry arguments forbid any moment to be present along *c*. A μ_{ferro} value of $0.002\mu_B$ was obtained and the sublattice magnetisation was found to be $5.0\mu_B$ (i.e. *gS*) which compares to $4.61\mu_B$ found by Epstein et al. [29]. The origin of spin canting was ascribed mainly to Dzyaloshinsky–Moriya (DM) antisymmetric exchange rather than to single ion magnetic anisotropy since the tilting of the Mn octahedral makes it difficult to see how this will cause moments to order in the *ab* plane. The DM mechanism also supports the value of the canting angle.

The $H(T)$ magnetic phase diagrams show spin–flop (SF)/antiferromagnetic and antiferromagnetic/paramagnetic boundaries in α-Mn(dca)$_2$ where H_{SF} ($T = 0$ K) = 4.8 kOe [36]. Inelastic neutron scattering measurements on this compound have revealed spin-waves at $E = 1.5$ meV [37]. Muon-spin rotation studies showed strong muon-spin relaxation in the paramagnetic state due to low-frequency fluctuation of the electronic moments in the 10^9–10^{10} Hz range. The relaxation is larger for Mn(II) ($^5A_{1g}$) than for Co(II) ($^4T_{1g}$) and Ni(II) ($^3A_{2g}$) [30].

α-Cr(dca)$_2$ ($T_N = 47.0$ K) [38] and α-Fe(dca)$_2$ ($T_N = 19.0$ K) [15,32] are also canted-spin antiferromagnets, the Fe(II) compound displaying a very large coercive field of 17 800 Oe at 2 K which varies with temperature, particle shape and size and synthesis method and arises from particle shape and Fe(II) magnetic anisotropies [15]. Its maximum energy product, $(B \cdot H)_{max}$, of 16.6×10^6 G Oe is similar to that of the "hard" commercial $SmCo_5$ magnets. The canting angle for α-Fe(dca)$_2$ was estimated to be 7.2° [15]. The magnetic ordering below T_N was nicely confirmed by Mössbauer spectroscopy from which a magnetically split spectrum was observed at 4.2 K in zero applied-field (Fig. 2) [32]. Above T_N, at 77 K, the unsplit quadrupole doublet was fitted to typical high-spin octahedral Fe(II) values of isomer shift ($\delta = 1.21$ mm s^{-1}) and quadrupole splitting ($\Delta E_Q = 3.17$ mm s^{-1}). We see later the influence that network geometry and Lewis

Table 1
Summary of magnetic data for α-M(dca)$_2$ (CA, canted antiferromagnet; F, ferromagnet)

	Cr	Mn	Fe	Co	Ni	Cu
Reference(s)	[38]	[15,27,38]	[15,32]	[14–16]	[14–16]	[14–16]
Spin (S)	2	5/2	2	3/2	1	1/2
μ_{eff} (300 K)/μ_B	4.79	5.71	5.07	4.75	3.12	1.88
θ (K)	−154	−25	3.22	9.7	22.7	0.7
C (cm^3 K mol^{-1})		4.42	3.36	2.82	1.21	0.44
Type of order		CA	CA	F	F	F [a]
J (cm^{-1})	–	−0.2 [b]	–	0.98 [a]	1.75 [c]	–
Coercive field (Oe (2 K))	300	406	17 800	710	7975	
Remnant magnetisation (cm^3 Oe mol^{-1})	220	29–53	2792	8098	5975	
$T_{N(c)}$ (K)	47.0	16.0	19.0	9.0	21.0	<1.7
Canting angle (°)		0.05	7.2			
Neutron diffraction; ordered sub-lattice magnetisation $\langle\mu\rangle$ per M/μ_B (T = 2 K)		5.0	4.12	2.54	1.68	

[a] Ref. [39].
[b] Ref. [29] (mean field theory).
[c] Ref. [39] (spin-wave theory).

base coordination (or clathration) has on these ^{57}Fe Mössbauer parameters. Neutron diffraction studies on α-Fe(dca)$_2$ confirmed the spin-canting with the two Fe moments restricted to the *ab* plane, their components along *a* being antiferromagnetically related while a small canting along *b* gives the observed ferromagnetism. The sublattice magnetisation μ(Fe) = 4.12μ_B gives the μ_{ferro} along *b* of 1.01μ_B [35].

α-Co(dca)$_2$ and α-Ni(dca)$_2$ show ferromagnetic order with T_C values of 9.0 and 21.0 K, respectively [14–16]. The coercive field for the Ni complex is very large and larger than for the Co complex [15]. It has a larger energy product (26.0×10^6 G Oe) than for α-Fe(dca)$_2$. Neutron powder diffraction studies of the low temperature magnetic structure of the Co and Ni complexes show collinear ferromagnetism with spin orientation along the *c*-axis [28]. There is no spin-canting in these ferromagnets. Muon-spin relaxation studies show strongly damped oscillations below T_C in the α-Co(dca)$_2$ case from which information on dynamical effects was gleaned [30]. Lappas et al. found agreement in the magnetic structure in their neutron powder diffraction studies but with some discrepancies in μ_{Co} and μ_{Ni} values. They also studied mixed species α-[$Co_{0.5}Ni_{0.5}$(dca)$_2$] and α-[$Fe_{0.5}Ni_{0.5}$(dca)$_2$], the former, as expected, being a collinear ferromagnet (T_c = 18.0 K), and the latter not showing long-range order [35].

The AC susceptibilities, χ' and χ'', were investigated as a function of applied pressure for α-M(dca)$_2$, M = Fe, Co, Ni [34]. The results yielded information pertinent to understanding the mechanism of long-range order (i.e. superexchange pathways leading to canted spin antiferromagnet (Fe) vs. ferromagnets (Co, Ni); see below). Application of pressure (1 bar to 18 kbar) displaces the T_C or T_N values (max in χ') and also broadens the peak in the same order as the single-ion anisotropy, i.e. Ni < Co < Fe. The broadening for the Fe complex at high pressure makes the maximum in χ' difficult to detect. The pressure dependence of the T_C (or T_N) values is quite marked and diverse, displaying a linear increase (6%) for Ni, a small increase followed by a decrease for Co, and a continued increase (up to 26% at 17 kbar) for Fe. These effects were rationalised in terms of electronic configuration and superexchange pathway/overlap differences. While there were early hints of weak spin-coupling in α-Cu(dca)$_2$ [16], it is only recently that ferromagnetic order has been observed by means of field dependent specific heat measurements [39]. In this paper the J values for α-M(dca)$_2$, M = Co, Ni were obtained from magnetic specific heat data, and fitting to various theoretical models for these Ising-like ions. The values are given in Table 1.

This brings us to one of the fascinating aspects of this rutile-like series. Why are the Cr, Mn and Fe species canted antiferromagnets, and the Co, Ni and Cu species ferromagnets? Structurally they are the same (or similar) and have doubly dca-bridged metals forming chains with adjacent chains being nearly orthogonal to each other. The d^n configuration, and hence the $t_{2g}^x e_g^y$ ligand-field configuration, changes along the series Cr(d^4), Mn(d^5), Fe(d^6), Co(d^7), Ni(d^8), Cu(d^9). Kurmoo [27,34] employed a Goodenough-type [40] superexchange model for rutile involving four nearest neighbour exchange interactions, three of which (J_a, J_b, J_c) are along the principal *a*, *b*, *c* axes (two for each M centre) and one (J_d) along the diagonal axes in the unit cell (eight for each M). The J_d interaction, along the M–N≡C–N–M (amide) pathway, is dominant. The other three involve Mn–N≡C–N–C≡N–M bridges and these are known to give very weak coupling (see later). The contributions to J_d arise from a number of overlaps between ligand and metal 'magnetic' orbitals. Experimentally, it is known that increasing the holes in t_{2g}^6 (i.e. Ni($t_{2g}^6 e_g^2$) to Mn($t_{2g}^3 e_g^2$)) gives more antiferromagnetic character, i.e. t_{2g}–e_g overlap leads to antiferromagnetic coupling, t_{2g}–t_{2g} ferromagnetic and e_g–e_g ferromagnetic (note that these are different to the μ-CN^- and μ-$C_2O_4^{2-}$ heterometallic systems where t_{2g}–e_g leads to ferromagnetic coupling [10,12]). The relative magnitude (ratio) of these exchange coupling terms will determine the nature of the coupled ground state. Jahn–Teller

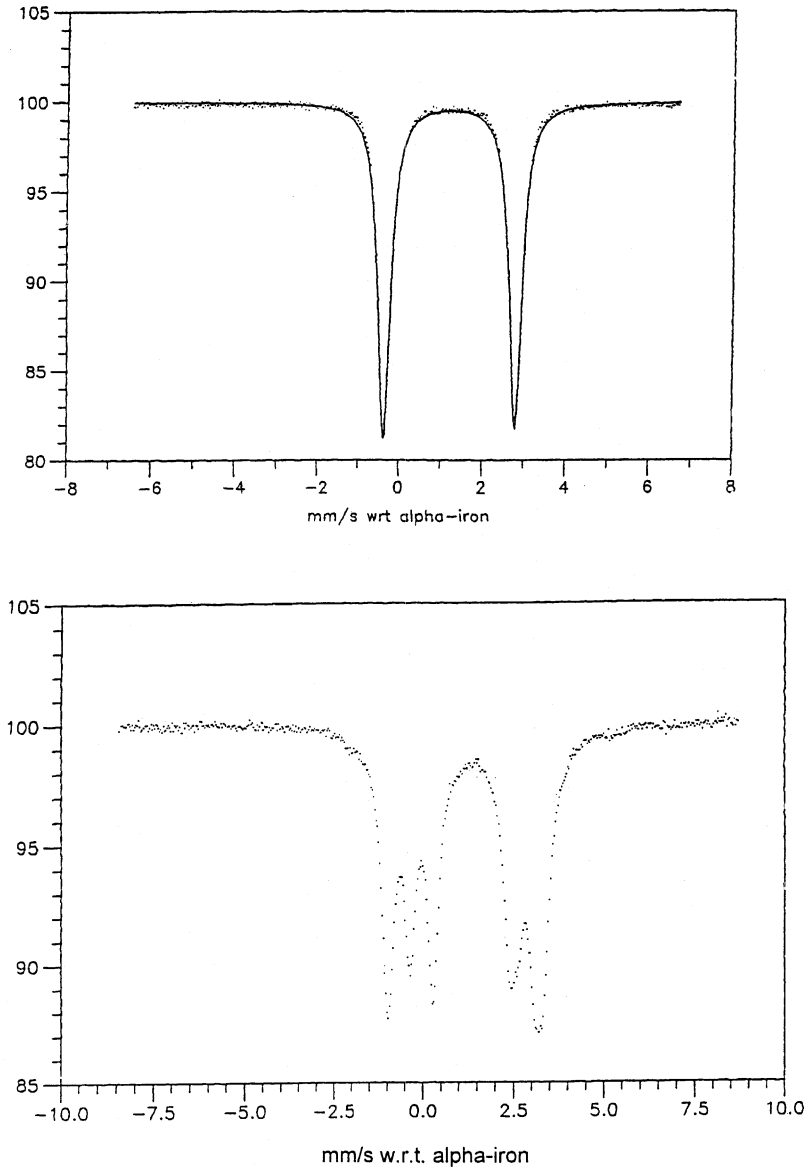

Fig. 2. Mössbauer spectra for α-Fe(dca)$_2$ measured at 77 K (top) and 2 K (bottom). The fit of the top spectrum yielded the isomer shift and quadrupole splitting values given in the text. The nature of the splitting in the bottom spectrum shows that the sign of the quadrupole splitting is negative. The internal hyperfine field is ca. 3 T.

elongation along the Cu–N(amide) bond in α-Cu(dca)$_2$ weakens the J_d interaction thus leading to paramagnetic behaviour above 1.7 K and ferromagnetic below 1.7 K [39]. J_d is strong and positive in the ferromagnets M = Co, Ni. The $t_{2g}^4e_g^2$ configuration in α-Fe(dca)$_2$ will give an equivalent number of ferro- and antiferromagnetic interactions, the latter being largest. Kurmoo predicted α-V(dca)$_2$ (t_{2g}^3) to be a ferromagnet in view of the t_{2g}–t_{2g} coupling [27,34].

Using Anderson [41], Goodenough [40] and Kanamori's [42] rules, Miller and Epstein and co-workers [29] proposed that a crossover from non-collinear antiferromagnetism (M = Cr, Mn, Fe) to collinear ferromagnetism (M = Co, Ni) occurs for a superexchange angle, α_c, of 142°. This tilting angle, between M···C···M atoms (i.e. superexchange via N–C≡N unit), was thought to be the dominant superexchange angle responsible for controlling the magnetism. However, the observation by Lappas et al. [35] of no ordering in α-[Fe$_{0.5}$Ni$_{0.5}$(dca)$_2$] ($\alpha_c = 141.73°$ at 1.7 K) but only enhanced short-range ferromagnetic coupling compared with α-[Fe(dca)$_2$], demonstrates that factors other than α_c must play a part in determining the magnetic ground state. One of the authors later expressed caution in the tilting angle explanation [43].

Ruiz et al. [44] have recently carried out theoretical calculations on the α-M(dca)$_2$ series using density functional theory to obtain J values and magnetostructural correlations. The $\mu_{1,3}$ M–N≡C–N–M pathway was found to provide the stronger coupling, as was predicted in the Goodenough

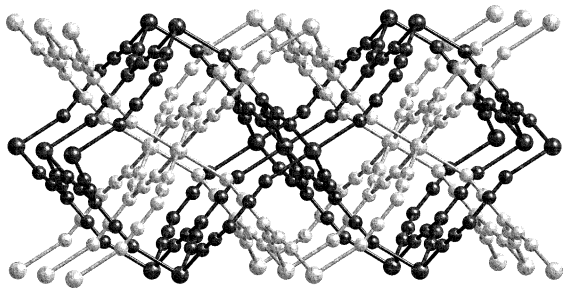

Fig. 3. The two interpenetrating 3D rutile-like networks in the structures of $M(tcm)_2$. The metal atoms are represented by the larger spheres.

model [34]. J values were calculated to be negative (antiferromagnetic) for V(II), Cr(II), Mn(II) and Fe(II), and positive for Co(II), Ni(II) and Cu(II), the value for Cu(II) being close to zero. The general agreement with experimental data is good and the agreement with J values obtained from mean field theory or spin-wave theory (Table 1) is reasonable. The V(II) calculation contradicts predictions from the Goodenough model [34].

The structures of $M(tcm)_2$, M = Cr, Mn, Fe, Co, Ni, Cu, Zn, Cd, Hg also form rutile-related networks, with octahedral metal ions and $\mu_{1,5,7}$ bridging tcm anions [45–49]. However, the larger size of the tcm ligand means that the networks are more spacious, such that two networks interpenetrate (Fig. 3). From a topological point of view, the smallest rings in the networks are four-membered $M_2(tcm)_2$ and six-membered $M_3(tcm)_3$ circuits (only the nodes, which are the metal ions and the central carbons of the tcm anions, are counted). The interpenetration is such that the six-membered rings of one net are penetrated by tcm anions of the second net, and vice versa. The four-membered rings are too small to be penetrated. The networks also show considerable distortion, indicating that the interpenetration results in a very tightly packed structure. The densities of the tcm networks, however, are comparable to their dca analogues, indicating that the packing in the latter structures is also very efficient. Another consequence of the interpenetration is the fact that the closest internetwork M···M distances are significantly shorter than the intranetwork ones.

The magnetic susceptibility data for the high-spin $M(tcm)_2$ series are generally indicative of weak antiferromagnetic coupling with no clear evidence for long-range order. The Weiss constants are Cr −31.2, Mn −5.1, Fe −25.0, Co −5.4, Ni −3.7, Cu −1.7 K [46]. The Cr system yielded $J = -1.6$ cm^{-1}, $zJ' = +0.04$ cm^{-1} when fitted to a $S = 2$ linear chain model modified to include chain–chain (zJ') coupling. Weak ferromagnetic interactions were evident in $Co(tcm)_2$ from field dependent studies of μ_{Co} below 20 K. A combination of magnetisation, specific heat and neutron diffraction measurements on $Cr(tcm)_2$ showed that long-range antiferromagnetic order occurs, with $T_N = 6.1$ K and moments aligned parallel to c [49]. $V(tcm)_2$ did not order but showed weak antiferromagnetic coupling [49]. EPR and magnetisation studies on $Cu(tcm)_2$ and $Mn(tcm)_2$ confirmed our observation of weak antiferromagnetic coupling but with evidence for antiferromagnetic order, at $T_N = 5.0$ K [48]. A recent neutron diffraction study on $Mn(tcm)_2$ measured at 0.04 K did not observe a 5 K transition but yielded the detailed magnetic structure, showing frustrated triangular ordering of the 'row model' type. In combination with specific heat data, the ordering temperature T_N was found to be 1.18 K. Unusual field dependence of the ordering was observed which implied the existence of three different field dependent phases [50].

The use of both dca and tcm ligands results in the synthesis of M(dca)(tcm), M = Co, Ni, Cu [51]. These compounds are both a structural and magnetic compromise between the $M(dca)_2$ and $M(tcm)_2$ 'parent' compounds. The structure contains octahedral metal ions and three-connecting $\mu_{1,3,5}$-dca and $\mu_{1,5,7}$-tcm ligands. The network formed is closely related to that of rutile—indeed, it has the same Schäfli symbol. In the rutile-related $M(tcm)_2$ and $M(dca)_2$ structures square channels are formed, with metal ions lying on the edges and ligands on the sides. Due to the different sizes of the ligands, however, in M(dca)(tcm) a helical substructure is formed instead of a square channel (Fig. 4), resulting in a self-penetrating network. The single self-penetrating network, closely related to but different from the rutile net, is a compromise between the single rutile network of $M(dca)_2$ and the doubly interpenetrating rutile networks of $M(tcm)_2$. Co(dca)(tcm) and Ni(dca)(tcm) display ferromagnetic ordering with $T_c = 3.5$ and 8.0 K, respectively [51]. Hysteresis data show that they are soft-magnets. The T_c values are lower than those of the α-$M(dca)_2$ analogues, however, the $M(tcm)_2$ 'parent' compounds show no long-range ordering for Co and Ni.

The syntheses of the M(dca)(tcm) compounds were inspired by the structure of $Mn(dca)_2(H_2O)$ [51]. This compound contains water molecules bound to Mn cations, and two types of dca ligands—one with a $\mu_{1,5}$ bridging mode, the other $\mu_{1,3,5}$. The $\mu_{1,3,5}$-dca ligands have the same function as those in the M(dca)(tcm) compounds. The

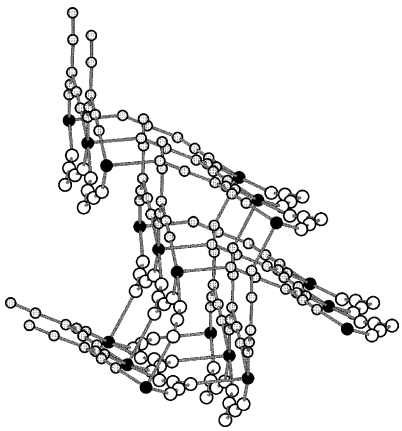

Fig. 4. A portion of the self-penetrating 3D net contained in the structures of M(dca)(tcm). Metal atoms are black, tcm atoms are grey, and dca atoms are white.

structural role of the tcm ligand is assumed by a $H_2O \cdot dca$ moiety in the hydrate structure. In this moiety the water is coordinated to the Mn and hydrogen bonds to the amide nitrogen of the $\mu_{1,5}$-dca ligand. Thus three Mn atoms are connected, two directly by the dca ligand, and the third via the hydrogen bond to the water ligand. This moiety lies across a mirror plane such that one of the NCN–M subunits is superimposed by symmetry onto the $N\cdots H_2O$–M subunit, and vice versa. Inspection of this disordered $dca \cdot H_2O$ moiety immediately brings to mind the tcm ligand, and in a true example of 'crystal engineering', it was shown that the same network could be generated by introducing tcm to the reaction mixture to replace the $dca \cdot H_2O$ substructure. Indeed, the M(dca)(tcm) compounds even crystallise in the same space group as the hydrate.

$Mn(dca)_2(H_2O)$ is a canted spin antiferromagnet with $T_N = 6.3$ K [51]. It was first observed in trace quantities in studies of α-[$Mn(dca)_2$] where it gave a small deflection at 6.3 K in the FCM and the specific heat plots [27]. The spin canting primarily arises because of the adjacent MnN_6 octahedra being disposed at 60.6° to each other along the N_{amide}-bridged pathways. Neutron diffraction studies would be required to obtain the magnetic structure in this orthorhombic *Ama2* phase and in the M(dca)(tcm) materials.

A second polymorph, the β-form, can also be formed by $M(dca)_2$ compounds. The structure of β-$Zn(dca)_2$ displays a 2D (4,4) sheet structure (Fig. 5), in which tetrahedral metal ions are bridged by $\mu_{1,5}$-dca ligands [26,52]. The kinked nature of the dca bridge, aided by some bending at the coordinating nitrogen donor atoms, allows the tetrahedral metal ions to be bridged into a corrugated square-grid sheet structure. The sheets stack in an interdigitated fashion, such that the shortest $Zn\cdots Zn$ distances are between sheets (4.45 Å) rather than within sheets (shortest distances, via the dca bridges, are 7.58 and 7.61 Å).

Blue crystals of a mixed-metal solid solution phase, in which Zn is doped with 0.12% Co, have also been formed [26]; the structure is isomorphous with the 100% Zn phase. Mixed metal solid solutions can also be made for the $M(tcm)_2$ and α-$M(dca)_2$ series of compounds [35,46].

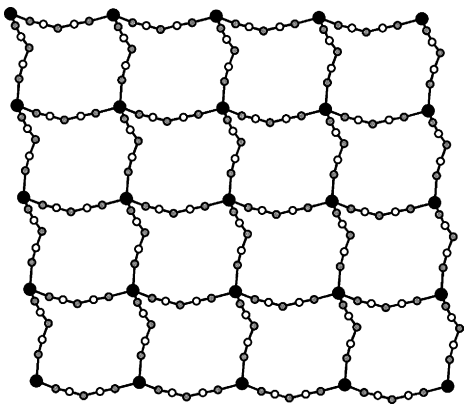

Fig. 5. The 2D (4,4) sheet structure of β-$M(dca)_2$. Atom shading as for Fig. 1.

A second phase of $Co(dca)_2$, the β phase, can be formed by depyridination under vacuum of $Co(dca)_2(pyridine)_2$ [16,26]. This product forms as a deep blue powder, and the visible spectrum is identical to that of the Co doped β-$Zn(dca)_2$ described above. On the basis of this and a very weak powder diffraction pattern for this compound, it is believed that β-$Co(dca)_2$ is isomorphous with β-$Zn(dca)_2$. Upon exposure to the atmosphere the powder turns from blue to pink, indicating a likely transformation to the α phase.

The deep blue Co(II) complex is a canted spin antiferromagnet with $T_N = 9.0$ K and values at 2 K of $H_c = 538$ Oe, RM = 0.22 Nβ [16,26]. The doped sample of 0.12% β-Co/$Zn(dca)_2$ was magnetically dilute, with $\mu_{eff} = 4.6\mu_B$ independent of temperature [26]. A second transition was observed at $T_N = 2.7$ K with glassiness implied from the FCM and ZFCM versus temperature data [16]. The change from ferromagnetic coupling in α-$Co(dca)_2$ to antiferromagnetic coupling in β-$Co(dca)_2$ primarily relates to changes from $\mu_{1,3,5}$ to $\mu_{1,5}$-dca bridging and different Co(II) ion ground states. The magnetic anisotropies on octahedral and tetrahedral Co(II) centres are markedly different and this may lead to spin-canting in the β-isomer.

2.2. Non-magnetic systems

A number of other diamagnetic simple binary metal salts of dca and tcm have also been reported. The structure of $Pb(dca)_2$ contains a complicated 3D network of nine-coordinate Pb atoms bridged by $\mu_{1,1,3,5}$ and $\mu_{1,1,3,5,5}$-dca ligands [53]. The compound Ag(dca) comes in both trigonal [54] and orthorhombic [55] modifications; both structures contain 1D chains of metal ions bridged by $\mu_{1,5}$-dca ligands which have helical and zigzag geometries, respectively. The structure of Ag(tcm) [56,57] contains pyramidal three-coordinate Ag ions bridged by $\mu_{1,5,7}$ tcm ions. 2D (6,3) sheets are generated, and layers of doubly interpenetrating sheets are formed. The structure of Ag(tcm)(MeCN) has a similar structure, with the now tetrahedral silver atoms also coordinating to terminal acetonitrile ligands [58]. $Hg_2(tcm)_2$ has a 3D network of $(Hg_2)^{2+}$ dimers bridged by $\mu_{1,5,7}$ tcm anions [59].

The structures of the alkaline earth metal salts $M(dca)_2$, M = Mg, Ca, Sr, Ba have been reported [60]. $Mg(dca)_2$ is isomorphous with the rutile-like α phase of the transition metal salts. In the isomorphous 3D structures of the Ca and Sr salts each metal is surrounded by eight nitrogen atoms, while each dca has a $\mu_{1,1,3,5}$ bridging mode. The Ba salt is isostructural with the Pb derivative described above. A number of alkali metal salts of dca [61] and tcm [62] have also been characterised crystallographically; the dca anions have been found to trimerise at elevated temperatures.

3. Coordination polymers with terminal coligands

To further explore the relationships between structure and magnetism in metal–dca coordination polymers it is useful

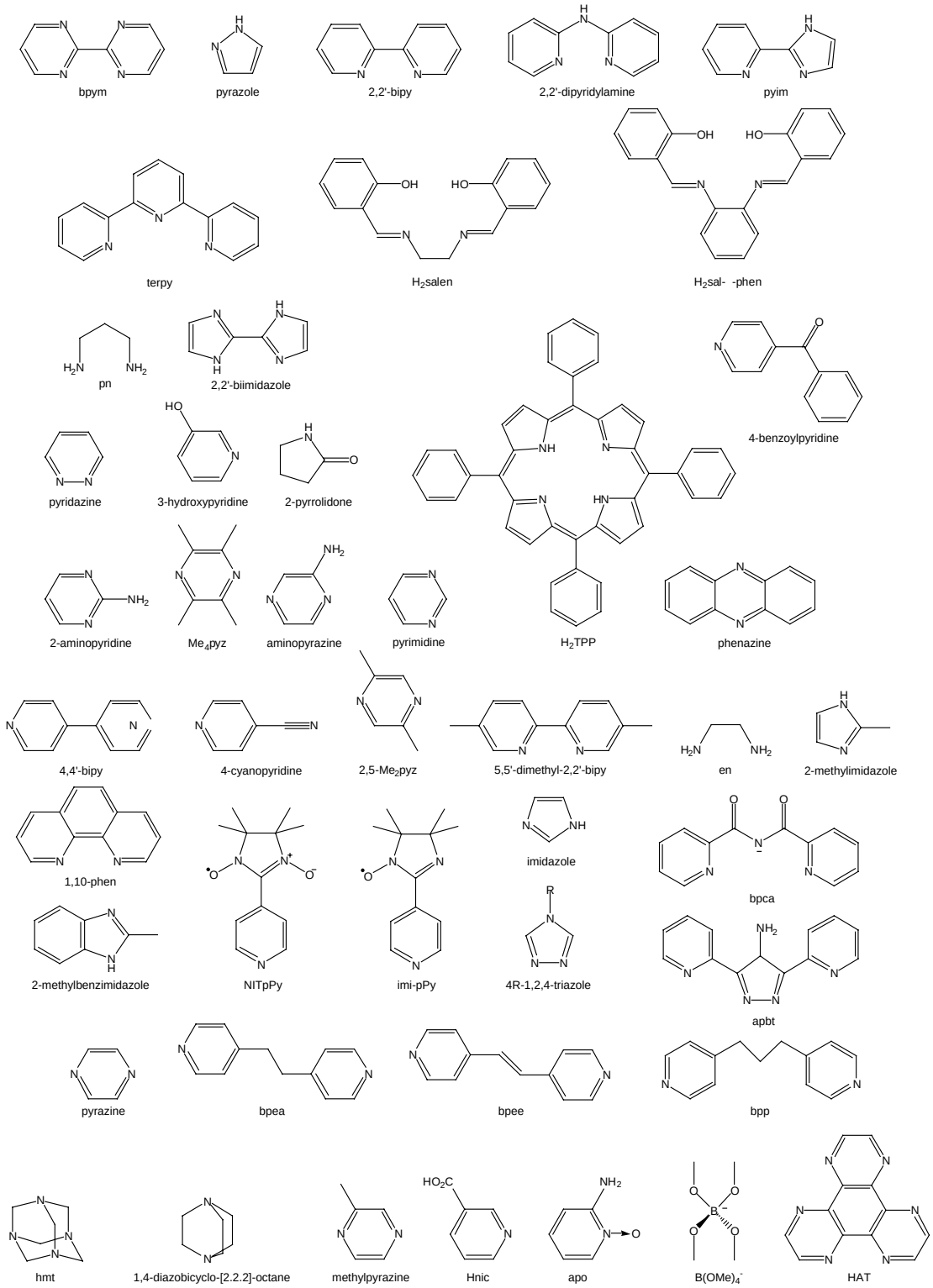

Scheme 3. Selected coligands contained in dca and tcm coordination polymers.

to have a variety of network topologies and dca binding modes to draw upon. One way of modifying the network topology is to introduce coligands into the structure. These ligands (Scheme 3) can either act as terminal non-bridging ligands whose main function is to occupy certain portions of the metal coordination sphere, or they may act as bridges themselves and, in the process, increase the dimensionality from 1D to 2D or 3D.

In this section we will look at structures that contain terminal ligands, beginning with 1D polymers, then working our way through 2D to 3D networks.

3.1. 1D networks

The simplest 1D networks are those that contain only one bridging dca per metal. These chains generally have either a linear or zigzag geometry, and are usually formed with bidentate or tridentate chelating coligands. There is much current interest in the magnetochemistry of chain systems such as those of the Haldane type containing even-spin metal ions such as Ni(II) or Mn(III) [63], and those of the so-called 'single chain magnet' type [64].

The compounds $M(dca)_2(bpym)\cdot H_2O$, M = Mn, Fe, Co, bpym = 2,2′-bipyrimidine [65] contain zigzag chains in which *cis* disposed $\mu_{1,5}$-dca ligands bridge metal ions whose octahedral coordination spheres are completed by chelating bpym and monodentate μ_1-dca and H_2O ligands. The metals show weak antiferromagnetic coupling across the dca bridges, the susceptibility data being fitted to a Fisher chain [66] model (Mn: $g = 2.04$, $\theta = -0.76$ K, $J/k_B = -0.15$ K; Fe: $g = 2.34$, $\theta = -7.6$ K, $J/k_B = -0.42$ K; Co: $g = 2.58$, $\theta = -5.4$ K, $J/k_B = -1.42$ K). The anhydrous complex $Mn(dca)_2(bpym)$ has a similar zigzag structure ($J/k_B = -0.27$ K, $g = 2.00$), but is bridged by double $\mu_{1,5}$-dca bridges [67]. It is isomorphous with the 2,2′-bipy complexes described below. This zigzag chain structure capped by *N*,*N*-chelators is well known in μ-oxalato systems [68]. The bpym ligand can itself also bridge between metal ions, and compounds in which it has this binding mode are discussed in the next section.

Linear chains of octahedral copper atoms are bridged by bidentate tcm anions in the structure of [*trans*-Cu(tcm)$(pyrazole)_4$](tcm) [69]. The structure also contains uncoordinated tcm counterions. ESR evidence pointed to weak exchange coupling. Curiously, data suggestive of ferromagnetic coupling and long-range antiferromagnetic ordering below 6 K were reported in the same paper for the compound $Cu(tcm)_2(pyrazole)_3$. This compound has a discrete molecular structure, with copper atoms coordinated to three pyrazole ligands and one monodentate tcm ligand, and bridged into dimers by two further bidentate tcm moieties. Further detailed magnetic studies are needed to confirm the ordering.

The copper(II) ion is often known to adopt five-coordinate geometry, and a number of chain compounds have been reported in which such copper atoms, which are also coordinated to chelating ligands, are bridged by $\mu_{1,5}$-dca ligands into 1D chains. $Cu(dca)_2L$, L = 2,2′-bipyridine (2,2′-bipy) [70,71] or 2,2′-dipyridylamine [72] also have monodentate μ_1-dca ligands, and show zigzag and linear geometries, respectively. No significant magnetic coupling was observed for the former compound, while weak intrachain antiferromagnetic coupling ($J = -0.10$ cm^{-1} for a $-J\mathbf{S_1}\cdot\mathbf{S_2}$ model of Hall [73]) was reported for the latter. In $[Cu(pyim)(dca)(H_2O)]NO_3$, pyim = 2-(2-pyridyl)imidazole the fifth coordination site is occupied by a water ligand (vs. monodentate dca in the previous two structures), and again weak antiferromagnetic coupling ($J = -0.35$ cm^{-1}) is observed for these zigzag chains [72].

Three chain structures have been reported with the tridentate chelating ligand 2,2′:6′,2″-terpyridine (terpy). Mn(terpy)(dca)(An), An = OAc^- [74,75] or NO_3^- [75,76] contain seven-coordinate metal atoms coordinated to tridentate terpy ligands, chelating OAc^- or NO_3^- anions, and two *trans* $\mu_{1,5}$-dca bridging ligands. The chains have zigzag geometries, and only weak antiferromagnetic coupling is observed ($J = -0.09$ and -0.12 cm^{-1}, respectively, for $-J\mathbf{S_1}\cdot\mathbf{S_2}$). The chains in the structure of $[Mn(terpy)(dca)(H_2O)]dca$ are linear, however, the structure also contains uncoordinated dca ligands which bridge the chains via hydrogen bonding interactions between the nitrile nitrogens and the coordinated water ligands, generating (4,4) sheets [76]. Again, only weak intrachain antiferromagnetic coupling ($J = -0.20$ cm^{-1}) is observed.

The tetradentate $salen^{2-}$ (*N*,*N*′-ethylenebis(salicylaldiminato)) ligand has been used to produce the 1D chain structures of M(salen)(dca), M = Mn(III), Fe(III) [75,77]. These are rare examples of M(III)–dca species and are related to M(salen)(OAc) chains [78]. The $\mu_{1,5}$-dca ligand bridges coordinate in a *trans* fashion, and weak antiferromagnetic intrachain coupling is observed. Shi et al. [77] assigned Mn(III) to be high-spin and Fe(III) to be low-spin using a Fisher chain model, deducing $J = -0.24$, -7.65 cm^{-1}, respectively. The data for the Fe(III) complex are clearly wrong and not representative of the high-spin structure. They probably have a sample containing some $(Fe(salen))_2O$. Their solution electrochemical data are meaningless since the chains do not exist in solution. We had earlier structurally characterised these $salen^{2-}$ complexes and the sal-*o*-$phen^{2-}$ (*N*,*N*′-*o*-phenylenebis(salicylaldiminato)) analogues, M^{III}(sal-*o*-phen)(dca). The fits of the magnetic data, using Fisher chain models for high-spin $S = 2$ (Mn) and $S = 5/2$ (Fe) gave: Mn(salen)(dca), $g = 1.91$, $J = -0.12$ cm^{-1}; Fe(salen)(dca), $g = 1.92$, $J = -0.12$ cm^{-1}; Mn(sal-*o*-phen)(dca), $g = 1.88$, $J = -1.85$ cm^{-1}; Fe(sal-*o*-phen)(dca), $g = 1.90$, $J = -0.72$ cm^{-1}. For comparison Mn(salen)(OAc) gave $g = 1.98$, $J = -1.8$ cm^{-1}, $zJ' = 0.1$ cm^{-1} [78] and Mn(salpn)(NCS), H_2salpn = *N*,*N*′-bis(salicylidene)-1,3-diaminopropane, gave $g = 1.99$, $J = -3.2$ cm^{-1} [79].

Fe(TPP)(tcm), H_2TPP = 5,10,15,20-tetraphenylporphyrin contains iron(III) porphyrin molecules bridged by $\mu_{1,5}$ tcm anions [80]. The structure of Mn(TPP)(dca)·THF is similar, with manganese(III) porphyrin molecules bridged into chains by $\mu_{1,5}$-dca anions [81]. The magnetic moment of this complex rises gradually from $4.57\mu_B$ at 300 K to $4.8\mu_B$ at 50 K, then more rapidly to reach a maximum of $5.7\mu_B$ at 5 K [81]. This is indicative of ferromagnetic coupling, a common feature of Mn(III) high-spin species. A *J* value of $+0.6$ cm^{-1} was obtained from a fit to a $S = 2$ Fisher chain model. The alternative explanation of crystallite orientation

effects and a negative D value being responsible for this increase in moment with decreasing temperature can be eliminated, since the data were reproducible under different fields [82]. Topologically, this complex is like the $\mu_{1,5}$ TCNE bridged compounds Mn(TPP)(TCNE) studied in detail by Miller et al. [83]. This class of compounds display ferrimagnetic chain behaviour ($S=2$ Mn(III); $S=1/2$ $TCNE^{\bullet -}$) with negative J (intrachain) values and long-range order observed, in some cases, with T_N values up to 28 K.

Other compounds to have linear chains containing one bridging dca ligand per metal include $Li(dca)(MeCN)_2$ [84] and $Cu(dca)(PPh_3)_2$ [85], both of which contain tetrahedral metals coordinated to two $\mu_{1,5}$-dca ligands and two monodentate ligands. $[Ni(dca)(pn)_2]ClO_4$, pn = 1,3-diaminopropane has metal centres coordinated to two chelating ligands and two *trans* $\mu_{1,5}$-dca bridges; only very weak antiferromagnetic coupling is observed [86]. Similar observations were recently made for the structure and magnetism of the octahedral high-spin d^7 system $[Co(dca)(2,2'\text{-biimidazole})_2]Cl$, which has a helical chain and imide–N(nitrile) binding ($g=2.22$, $D=40.3$ cm^{-1}, $zJ=-0.04$ cm^{-1} (intermolecular)) [53]. $Ru_2(OAc)_4L$, L = dca, tcm [87] contain $[Ru_2(OAc)_4]^+$ dimers bridged by $\mu_{1,5}$-dca or $\mu_{1,5}$ tcm ligands. Only very weak antiferromagnetic interactions were found to occur between the Ru_2 units through the dca ($g=2.16$, $zJ'=-0.33$ cm^{-1}) and tcm ($g=2.15$, $zJ'=-0.22$ cm^{-1}) bridges.

Chains formed by two bridging $\mu_{1,5}$-dca ligands per metal are much more common than those with only one per metal. Such chains with a linear geometry (i.e. a *trans* arrangement of terminal ligands) are particularly common. The structure of $Mn(dca)_2(pyridine)_2$ [27,88], shown in Fig. 6, is typical. The metal ions are bridged by four-equatorial dca ligands into a linear chain; each pair of adjacent metal ions is connected by a pair of dca ligands. The chains pack in an interdigitated fashion (Fig. 6), such that the terminal pyridine ligands associate in what looks initially like a π-stacked arrangement. However, the distances between the mean planes of the ligands (3.543 and 3.601 Å) are rather long. More significantly, the DMF derivative $Mn(dca)_2(DMF)_2$, in which the terminal ligands have no π system, displays an analogous interdigitated structure [27]. Thus the role of any π···π interactions in the pyridine derivative is minor, with the driving force for the interdigitation being the maximisation of packing efficiency. The interplanar distance between the pyridine rings is, of course, governed by the intrachain Mn···Mn repeat distance.

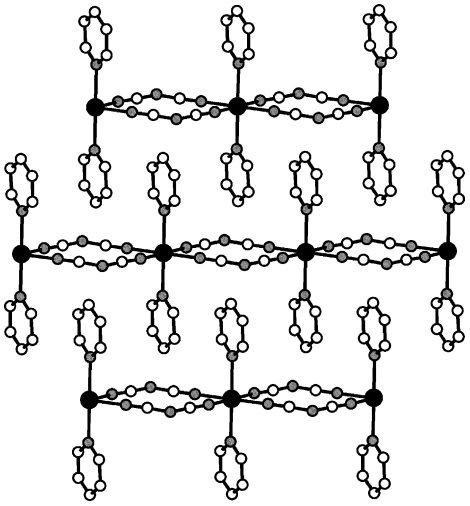

Fig. 6. The interdigitating linear chain structure of $M(dca)_2(pyridine)_2$. Atom shading as for Fig. 1.

The pyridine and DMF chains both display weak antiferromagnetic coupling between the metal ions ($J=-0.24$ cm^{-1} for both (using a $-J\mathbf{S_1}\cdot\mathbf{S_2}$ Fisher chain model [27])), as do the structurally analogous $Mn(dca)_2L_2$, L = pyridazine [74] ($J=-0.75$ cm^{-1}), 4-benzoylpyridine [89] ($J=-0.3$ cm^{-1}) and 2-pyrrolidone [90] ($J=-1.6$ cm^{-1}) compounds. The structures of $Co(dca)_2(2\text{-pyrrolidone})_2$ [90] and $Cd(dca)_2(pyridine)_2$ [91] are isomorphous with the Mn derivatives described above; the Co compound also shows antiferromagnetic coupling. The structure of $Cu(dca)_2(3\text{-hydroxypyridine})_2$ [92] has this linear chain topology, however, one of the Cu–N(dca) interactions is only very weak (2.967(3) Å).

The isomorphous structures of $M(dca)_2(MeOH)_2$, M = Fe [27,93], Mn [27] also have the linear chain topology described here, however, interchain hydrogen bonding interactions between the methanol and the uncoordinated amide nitrogen of the dca ligands give rise to 2D layers. Both compounds again only show weak antiferromagnetic coupling. The $S=2$ Fe(II) data were fitted to a chain model ($g=2.04$, $J/k_B=-0.23$ K) modified by a mean-field term $J'/k_B=-0.02$ K. Zero-field splitting also plays a part. There was no evidence of a Haldane gap. The structure of $Cu(dca)_2(2\text{-aminopyrimidine})_2$ has similar chains cross-linked by hydrogen bonding between the 2-aminopyrimidine ligands; no significant magnetic coupling is observed [94]. The Ni(II) and Co(II) analogues also show very weak antiferromagnetic coupling [95].

The structure of $Mn(dca)_2(H_2O)_2\cdot 2Me_4pyz$, Me_4pyz = tetramethylpyrazine contains 1D chains with *trans* water ligands [96]. The tetramethylpyrazine ligands hydrogen bond to the water ligands and form $\cdots Me_4pyz\cdots H_2O\cdots Me_4pyz\cdots H_2O\cdots$ chains which flank either side of the coordination polymer chains. Very weak intrachain antiferromagnetic coupling is observed ($J=-0.16$ cm^{-1}). The related tcm complexes $M(tcm)_2(H_2O)_2\cdot Me_4pyz$, M = Co, Ni contain similar chains of metal ions connected by double $\mu_{1,5}$ tcm bridges [97]. In this case, however, the chains are connected into a 3D network by hydrogen bonding interactions between the *trans* water ligands and the Me_4pyz molecules, and between the water molecules and the uncoordinated nitrogen atoms of the tcm anions. Both compounds showed very weak intrachain antiferromagnetic coupling, with a hint of interchain ferromagnetic coupling in the Ni case. Neither compound displays long-range ordering.

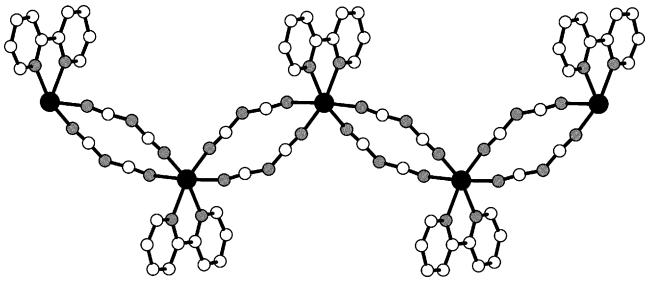

Fig. 7. The 1D zigzag chain in *cis*-M(dca)$_2$(2,2′-bipy). Atom shading as for Fig. 1.

The other form of chain that can be formed by compounds containing two bridging dca ligands per metal is that with the zigzag geometry. Only a few of these type have been reported to date, mainly with bidentate chelating ligands (although a *cis* arrangement of terminal ligands will also generate the same chain geometry). The isomorphous structures of *cis*-M(dca)$_2$(2,2′-bipy), M = Mn [88,89,98] or Cd [99], shown in Fig. 7, are indicative. Weak antiferromagnetic coupling only ($J = -0.4$ cm^{-1} using $-J\mathbf{S_1} \cdot \mathbf{S_2}$ [89]) is observed for the Mn derivative. Escuer et al. used superexchange calculations to compare $\mu_{1,5}$-dca and $\mu_{1,3}$ azide bridging, the latter being stronger due to the more efficient π pathways [89].

A small number of other 1D dca bridged coordination polymers with more unusual topologies has been reported. The structure of Mn(dca)$_2$(H$_2$O)(aminopyrazine) has a ladder-like motif, with $\mu_{1,5}$-dca ligands [100]. The rungs of the ladders are formed by double dca bridges, while the sides are formed by single dca bridges. The octahedral coordination sphere of the metal is completed by terminal aminopyrazine and water ligands. Weak antiferromagnetic coupling and zero-field splitting was noted without long-range order.

The structure of the 1D chains of Cu(dca)$_2$(2-aminopyrimidine)$_2$ has been mentioned above, and we also have the Co analogue, which forms 2D (4,4) inclined interpenetrated nets involving hydrogen bonding [95]. It shows monomer like magnetic moment behaviour. Another product, M(dca)$_2$(2-aminopyrimidine), M = Co, Ni can also be obtained by reaction of the two ligands with metal ions [101]. These latter products have a fascinating 1D tube-like network, which is shown in Fig. 8. The edges of these tubes are occupied by the octahedral metal ions, while the sides are formed by $\mu_{1,3,5}$-dca ligands. The coordination sites on the periphery of each tube are occupied by bridging $\mu_{1,5}$-dca ligands and terminal 2-aminopyrimidine ligands coordinating through one of the aromatic nitrogen atoms. The tubes are connected into a 3D net by intertube hydrogen bonding between the 2-aminopyrimidine ligands (NH$_2$ donor and aromatic N acceptor) and between the 2-aminopyrimidine ligands and the $\mu_{1,5}$-dca ligands (NH$_2$ donor and amide dca N acceptor). An interesting feature of the tubes is that the topology of the M–dca net is identical to that of the square channels in the rutile-like M(dca)$_2$ compounds mentioned in the previous section.

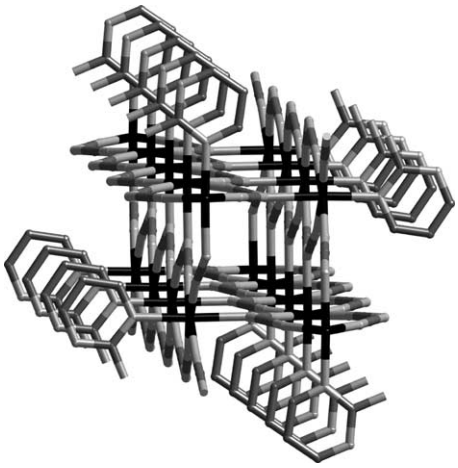

Fig. 8. A 1D tube from the structure of M(dca)$_2$(2-aminopyrimidine). Metal ions (black) lie on the edges of the tube, while $\mu_{1,3,5}$-dca ligands form the sides, and the periphery contains $\mu_{1,5}$-dca and 2-aminopyrimidine ligands.

The magnetism of these tube-like systems is intriguing and not yet fully understood. The $\mu_{1,3,5}$-dca bridging is expected to lead to stronger coupling than $\mu_{1,5}$ bridging and, as in α-Ni(dca)$_2$, ferromagnetic coupling is anticipated. This is so in Ni(dca)$_2$(2-aminopyrimidine) as evidenced by a gradual increase in μ_{eff} from $3.1\mu_B$ at 300 K to $4.9\mu_B$ at 3.6 K, before decreasing a little as the temperature is decreased to 2 K [101]. Increasing the field to 4 T leads to a broader maximum at lower μ_{eff} values. Such behaviour is reminiscent of Zeeman level depopulation effects within which M is not linear with H [102]. Use of small DC fields (20 and 200 Oe) gives a rapid increase in μ_{eff} below 20 K but not that typical of long-range order. AC susceptibility measurements and FCM and ZFCM DC data also do not yield bifurcation characteristic of magnetic order. Kurmoo [103] has calculated the 20 Oe data quite well using a Heisenberg model for short-range coupling assuming a Ni$_8$ fraction of the tube, with positive J values. The Co(II) analogue does not show long-range order but shows typical octahedral d^7 behaviour of μ_{Co} between 300 and 20 K, then goes through a minimum followed by a rapid increase to a sharp maximum of $4.9\mu_B$ at 4.4 K. Lower fields give even higher μ_{Co} values at 2 K. Very similar behaviour is displayed by Co(dca)$_2$(H$_2$O) · phenazine, described later with an interpretation. There are aspects of the above behaviour in the 3D network compounds M(dca)$_2$(pyrimidine) · EtOH (M = Fe, Co) but clear AC susceptibility and hysteresis evidence for long-range order ($T_N = 3.2$ K for the Fe(II) complex and 1.8 K for Co(II)) was obtained [104]. This is surprising for $\mu_{1,5}$-dca bridging (with $\mu_{1,3}$ pyrimidine). The isostructural Ni(dca)$_2$(pyrimidine) · H$_2$O is also a canted-spin antiferromagnet, with $T_N = 8.3$ K [105]. Cu(dca)$_2$(2-aminopyrimidine) shows Curie–Weiss behaviour indicative of weak antiferromagnetic coupling [95].

Tube-like 1D coordination networks (Fig. 9) are also formed in the structures of M(dca)$_2$(4,4′-bipy)(H$_2$O) ·

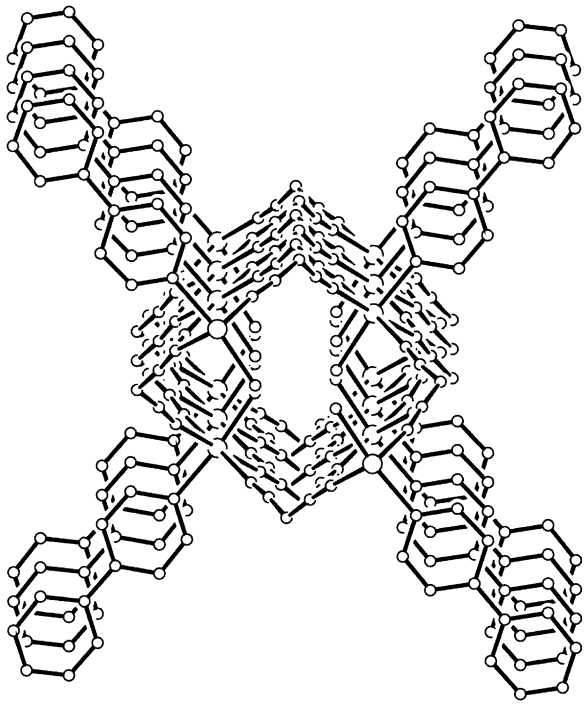

Fig. 9. A 1D tube from the structure of $M(dca)_2(4,4'\text{-bipy})(H_2O)\cdot solv$. Note the topology is different to the tube shown in Fig. 8. Metal ions (large circles) lie in the middle of the sides of the tube, while $\mu_{1,5}$-dca ligands form the edges and the rest of the sides. The terminal water ligands lie inside the tube (as do the solvent molecules, omitted here for clarity), while monodentate 4,4′-bipy ligands radiate out from the tube.

0.5MeOH, M = Mn, Fe, Co, 4,4′-bipy = 4,4′-bipyridine [106] and $M(dca)_2(4,4'\text{-bipy})(H_2O)\cdot 0.5H_2O$, M = Mn [88,98], Fe [107]. Although the 4,4′-bipy ligand can act as a bridging ligand (and does in other dca compounds, vide infra), in these compounds it is monodentate. The tube has a different topology to the 2-aminopyrimidine tubes described above. It contains only $\mu_{1,5}$ bridging dca ligands, with the metal ions sitting not at the edges but in the middle of the sides of the tubes. Each metal is coordinated to four of these bridging dca ligands in an equatorial arrangement, and the four dca ligands connect each metal to four other metal ions. The octahedral geometries of the metal ions are completed by terminal 4,4′-bipy ligands on the periphery of the tubes, and water ligands which lie in the interiors of the tubes. The tubes pack in the crystal structure such that the uncoordinated nitrogen atoms of the 4,4′-bipy ligands of each tube hydrogen bond to the interior water ligands of adjacent tubes, generating two interpenetrating 3D nets. The magnetic properties of the hemihydrate and hemimethanolate Mn(II) compounds are similar, typical of weak antiferromagnetic coupling and fitted to a $S = 5/2$ 1D Fisher chain ($-J\mathbf{S_1}\cdot\mathbf{S_2}$) model to yield $J = -0.33$ cm^{-1} ($0.5H_2O$) and $J = -0.21$ cm^{-1}. There were hints of long-range order occurring in the $0.5H_2O$ case but not in the 0.5MeOH case. The Fe(II) and Co(II) analogues showed very weak antiferromagnetic coupling as judged by powder susceptibilities and single crystal data on the anisotropic Co(II) complex [106].

3.2. 2D networks

Only a small number of compounds has been reported to contain 2D M–dca networks with non-bridging coligands. These structures, for the most part, have either (4,4) or (6,3) topology with bridging $\mu_{1,5}$-dca ligands. Those structures with (4,4) topology include $Mn(dca)_2$(4-cyanopyridine)$_2$ [108] and $Mn(dca)_2(EtOH)_2\cdot Me_2CO$ [27]. Both compounds have a *trans* arrangement of terminal ligands and show weak antiferromagnetic coupling. The 4-cyanopyridine data were fitted to 2D Curely [66b,109] or Lines [110] models yielding $g = 2.01$, $J = -0.17$ cm^{-1}. The compounds $M(tcm)_2(EtOH)_2$, M = Co, Ni have (4,4) sheet structures with bridging $\mu_{1,5}$ tcm anions, similar to the Mn–dca analogue [85]. There is also extensive intrasheet hydrogen bonding between the ethanol ligands and the uncoordinated arms of the tcm anions. The structure of $Mn(dca)_2(H_2O)_2\cdot 2$(2,5-Me_2pyz), 2,5-Me_2pyz = 2,5-dimethylpyrazine has similar sheets with water ligands occupying the axial positions on the metal ions [100]. The water ligands hydrogen bond to 2,5-Me_2pyz molecules that lie between the layers and connect them into a 3D network. Magnetic measurements show a spin canted phase transition at 1.78 K; the hydrogen bonding between layers may be important in this observation of long-range magnetic ordering.

The structure of $Cu(dca)_2$(5,5′-dimethyl-2,2′-bipy) also has (4,4) topology, but is slightly different to the above examples [111]. Each copper atom is coordinated to a single chelating ligand rather than two *trans* monodentate ligands, and one of the Cu–N(dca) links is only a weak interaction (3.006(2) Å).

2D sheets with (4,4) topology and bridging $\mu_{1,5}$-dca ligands are formed in the structure of $Me_2Sn(dca)_2$ [112]. The related structure of $Me_3Sn(dca)$ contains 1D chains of Me_3Sn^+ moieties bridged by *trans* $\mu_{1,5}$-dca ligands [112]. $Me_3Sn(tcm)(H_2O)$ is molecular, with monodentate tcm, however, hydrogen bonding interactions between the uncoordinated nitrile nitrogens of the tcm ligands and water ligands on adjacent molecules create 2D (6,3) networks [113].

The structure of $[Cu(en)_2][Mn(dca)_4]$, en = ethylenediamine contains dca ligands displaying both the $\mu_{1,5}$ and (the rare) $\mu_{1,3}$ bridging modes [114]. The Mn ions are bridged into linear chains by double $\mu_{1,5}$-dca ligands. The octahedral Mn coordination spheres are completed by *trans* dca ligands bonding through a nitrile nitrogen each. These dca ligands then crosslink the chains into sheets with (4,4) topology by binding via their amide nitrogen atoms in a *trans* fashion to $Cu(en)_2^+$ moieties. Despite the $\mu_{1,3}$ bridging mode, only weak antiferromagnetic coupling is observed ($J_{Mn} = -0.24$ cm^{-1}).

The compounds $M(tcm)_2$(2-methylimidazole)$_2$, M = Co [115], Cu [116] both contain octahedral metal ions coordinated to *trans* monodentate 2-methylimidazole ligands and bridged by bidentate tcm anions. The topologies of the networks formed, however, are very different. The Co structure

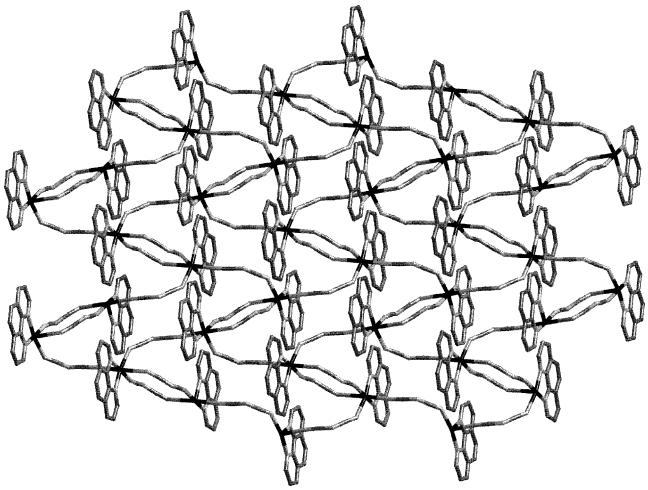

Fig. 10. The 2D (6,3) sheet topology of M(dca)$_2$(1,10-phen), M = Cu, Cd.

consists of linear 1D chains with double tcm bridges, while the Cu complex has 2D (4,4) sheet topology.

There have also been three M–dca structures reported with (6,3) topology. The structure of Cu(dca)(MeCN) is a rare example of a structure containing $\mu_{1,3,5}$-dca ligands, with the tetrahedral Cu(I) geometry completed by terminal acetonitrile ligands [117]. The isomorphous structures of M(dca)$_2$(1,10-phen), M = Cu [91,118], Cd [99] contain (6,3) sheets in which two thirds of the links are single $\mu_{1,5}$-dca bridges and one third of the links are double M($\mu_{1,5}$-dca)$_2$M connections (Fig. 10). The octahedral metal ion geometry is completed by the chelating 1,10-phenanthroline ligands. One of the Cu–N(dca) interactions in the Cu compound is weak (2.821(3) Å), and only weak coupling ($J = 0.2$ cm^{-1}) is reported, although, unusually, it is of a ferromagnetic nature [70]. This bears further scrutiny since the μ_{eff} value at room temperature (r.t.) was less than the spin-only value.

A number of compounds has been reported with radical coligands. The structure of Mn(NITpPy)$_4$(dca)$_2$, NITpPy = 2-(4-pyridyl)-4,4,5,5-tetramethylimidazoline-1-oxyl 3-oxide contains 1D linear chains of metal atoms connected by double $\mu_{1,5}$-dca bridges [119]. One type of NITpPy molecule coordinates in the axial metal positions, while the other type lie uncoordinated in the lattice. Only weak antiferromagnetic interactions are observed which are thought not to involve the radicals, but rather involve intrachain Mn···Mn interactions via the dca bridges. The structure of Cu(NITpPy)$_2$(dca)$_2$ · 3MeCN has similar chains but no uncoordinated NITpPy molecules in the lattice [120]. By contrast, the structure of Cu(NITpPy)$_2$(dca)$_2$ · 2MeCN contains 2D (4,4) sheets, even though the metal atoms are again bridged by $\mu_{1,5}$-dca ligands and the radical ligands again coordinate in a *trans* fashion [120]. The magnetic data for both Cu compounds are suggestive of ferromagnetic Cu···Cu interactions via the dca bridges at low temperatures (mean field $zJ' = +1$ cm^{-1}), however, the magnetic properties are dominated by Cu-(radical)$_2$ antiferromagnetic interactions, the latter simulated using a $-J\mathbf{S_1} \cdot \mathbf{S_2}$ linear $S = 1/2$ trimer model with $J = -15$ cm^{-1}. The Mn analogue of the Cu (4,4) sheet structure is isomorphous, and the magnetism is dominated by ferromagnetic Mn-radical interactions ($J = +3.9$ cm^{-1}); any coupling via the dca bridges is either very weakly antiferromagnetic or non-existent ($zJ' = -0.17$ cm^{-1}) [121]. The magnetic data bear further study, particularly by varying the field, since there are other possible reasons for sharp maxima occurring in μ_{eff} (or $\chi_m T$) versus T plots at low temperature. Finally, when the closely related radical ligand 2-(4-pyridyl)-4,4,5,5-tetramethylimidazoline-1-oxyl (imi-pPy) is used, the compound *cis*-Cu(imi-pPy)$_2$(dca)$_2$ is obtained [122]. This compound shows a 1D zigzag structure with double $\mu_{1,5}$-dca bridges between the metals and a *cis* arrangement of radical ligands. Again, the metal–radical interactions dominate the magnetic data, and only weak antiferromagnetic interactions via the dca bridges are reported.

In our work on the M(dca)$_2$–Lewis base adducts we employed sterically hindered bases such as phenazine, which is also well known to act as an intercalator. The M–dca networks in the structures of M(dca)$_2$(H$_2$O) · phenazine, M = Fe, Co, Ni [123] show the very interesting topology displayed in Fig. 11. The structure contains both $\mu_{1,5}$ and $\mu_{1,3,5}$-dca ligands, as well as two types of metal ions. One type of metal bonds to six dca ligands (four-equatorial $\mu_{1,5}$-dca ligands and two axial $\mu_{1,3,5}$-dca ligands coordinating via the amide nitrogens), while the other bonds to four-equatorial $\mu_{1,3,5}$-dca ligands (via the nitrile nitrogens) and two axial water ligands. In the crystal packing these M(dca)$_2$(H$_2$O) sheets alternate with layers of phenazine molecules which hydrogen bond to the water ligands of the sheets and bridge them into a 3D network. The topology of the sheets is very significant in that it is identical to a 2D substructure that can be defined in the rutile structures of α-M(dca)$_2$ (which, as mentioned previously, show long-range magnetic ordering). In fact, the α-M(dca)$_2$ structure can be generated by removing the phenazine and

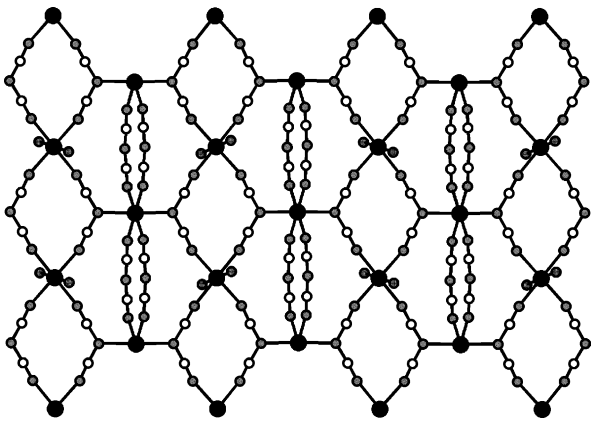

Fig. 11. A single M(dca)$_2$(H$_2$O) sheet from the structure of M(dca)$_2$(H$_2$O) · phenazine. Note the two different dca bridging modes, and the two different metal coordination environments. Atom shading as for Fig. 1.

water molecules, and moving the sheets such that the amide nitrogens of the $\mu_{1,5}$-dca ligands come to occupy the coordination sites previously occupied by the water ligands.

Interestingly, the structures of these phenazine derivatives are also reminiscent of the Mn–2,5-Me_2pyz structure described above [100]. In all these structures the uncoordinated heterocyclic Lewis bases hydrogen bond to water ligands in the layers, connecting them into 3D networks. The steric bulk of both ligands no doubt plays a role in preventing their direct coordination to the metal ions. It is also useful to note that both compounds are to date the only ones with terminal coligands (defined by only considering coordination bonds) to show long-range magnetic ordering, indicating that hydrogen bonding bridging pathways are perhaps important in such phenomena.

The Fe(II) and Ni(II) phenazine derivatives give clear evidence for long-range magnetic order, no doubt influenced by the stronger coupling provided by the $\mu_{1,3}$-dca bridging moieties. Magnetisation contributions from traces of α-[Ni(dca)$_2$] were observed in the Ni(II) data and were easily identified in relation to a ferromagnetic transition at 5.7 K followed by 3D antiferromagnetic order below 5 K. At 2 K, H_c is 65 Oe and RM is 3177 cm^3 mol^{-1} Oe, which is indicative of a soft ferromagnet.

The Fe(II) complex gives a clear bifurcation in the FCM and ZFCM plots at $T_c = 4.5$ K (Fig. 12). The AC χ' data, determined at 10 Hz, shows a rapid increase below 5 K with a maximum at 4.5 K, then a more gradual decrease such that χ' does not reach zero at 2 K. This is not a typical shape of χ' versus T for a ferromagnet but such shapes have recently been seen in a layered Ni_3Fe_2 μ-cyano ferromagnet [124] and assigned to the dynamics of magnetic domains in the ordered phase. The hysteresis loop of the present compound is typical of a soft ferromagnet. The M versus H isotherm at 2 K shows a rapid increase at very low fields then a gradual, slow increase reaching $M = 2.9$ Nβ at 5 T. Further confirmation for the ordered phase came from the zero-field Mössbauer spectra in which the two quadrupole doublets at 77 K gave a magnetically split hyperfine pattern below T_c (at 2 K).

Our earlier report [123] on Fe(dca)$_2$(H_2O) · phenazine mentioned a separate layered structure, Fe(dca)$_2$(H_2O)$_2$ · 2phenazine · 2EtOH, which also contained intercalated phenazine held between $\mu_{1,5}$-dca doubly-bridged chains of Fe(H_2O)$_2$. The magnetic ordering reported at 4.5 K is now known to be due to contaminating Fe(dca)$_2$(H_2O) · phenazine [125].

In contrast to Fe and Ni, the Co(II) phenazine complex gives no clear evidence for long-range order, i.e. no bifurcation in FCM and ZFCM. In a field of 1 T, the observed decrease in μ_{Co} from 4.84μ_B at 300 K to 4.20μ_B at 20 K, followed by an increase to a maximum in μ_{Co} of 4.52μ_B at 4.3 K (Fig. 13), is a reasonably common 'minimax' μ_{Co}/T motif in polymeric Co(dca)$_2$(2-aminopyrimidine) [101] and Co(tcm)$_2$ [46] species. It derives from the effect of

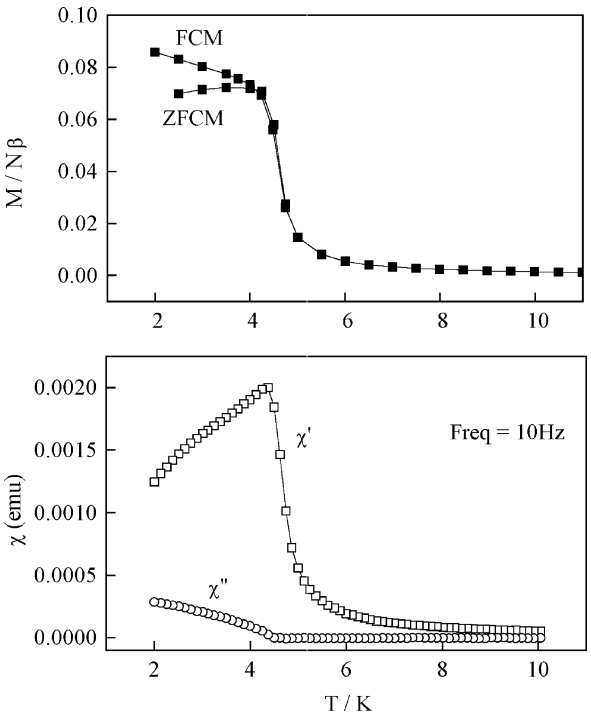

Fig. 12. Top: Plots of field cooled and zero field cooled magnetization vs. temperature for Fe(dca)$_2$(H_2O) · phenazine. Bottom: Plots of AC in-phase (χ') and out of phase (χ'') susceptibilities for Fe(dca)$_2$(H_2O) · phenazine.

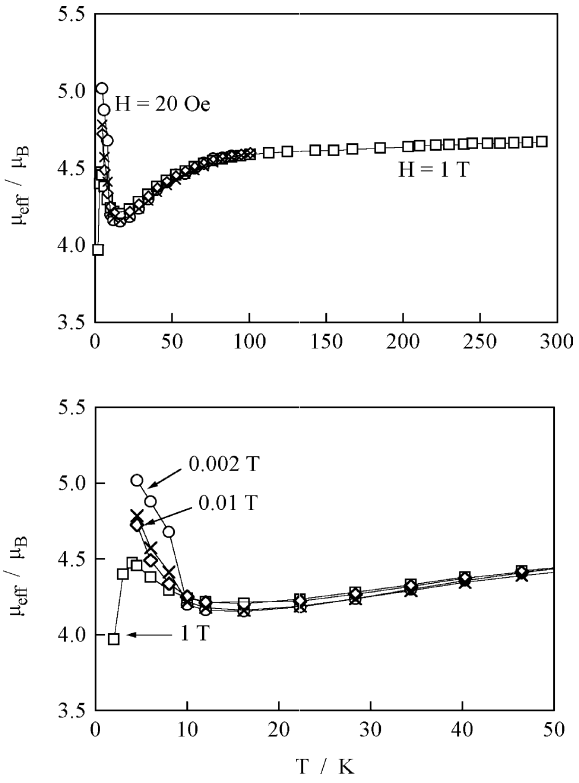

Fig. 13. Top: Plots of magnetic moment, per Co, vs. temperature for Co(dca)$_2$(H_2O) · phenazine in fields of 1 T (squares) and 20 Oe (circles). Bottom: Expansion of the 2–50 K region in fields varying from 1 T to 20 Oe.

spin–orbit coupling and low-symmetry ligand field splittings on single-ion $^4T_{1g}$ states combined with weak ferromagnetic coupling between such ions. Thermal depopulation of the resulting Zeeman levels yields the unusual temperature dependence of μ_{Co} at different field values. The exchange coupling is presumably not strong enough to overcome single ion effects and yield the long-range order displayed by the 3D ferromagnet α-Co(dca)$_2$ [14–16] and by the layered, hard ferrimagnet $Co^{II}_5(OH)_8(dca)_2 \cdot 6H_2O$, although the latter is dominated by intra-layer (cobalt-hydroxide) coupling rather than by inter-layer coupling, via the dca bridges [126,127].

Another very unusual structure with terminal coligands is that of Mn(dca)$_2$(H$_2$O)$_2 \cdot$ H$_2$O [27,33a]. This compound contains both 1D chains and 2D sheets of the same composition (Mn(dca)$_2$(H$_2$O)$_2$), each containing $\mu_{1,5}$-dca bridges and metal coordination spheres composed of four-equatorial dca and two axial water ligands. The 2D sheets have (4,4) topology, and stack such that the windows of the sheets align and create channels. The linear 1D chains, in which the metals are connected by double dca bridges, lie in these channels. The structure also contains intercalated water molecules, and between the sheets there are complicated 2D hydrogen bonding networks involving the intercalated water molecules, the coordinated water ligands, and the uncoordinated amide nitrogen atoms of the dca ligands. The magnetic data indicates only very weak antiferromagnetic coupling. Another hydrate structure, Mn(dca)$_2$(H$_2$O), was mentioned earlier in conjunction with the M(dca)(tcm) compounds [51].

3.3. 3D networks

Only two 3D M–dca networks have been reported to date with terminal coligands. The first such structure is that of Me$_2$Tl(dca) [128]. The dca ligand in this complex shows an unusual $\mu_{1,1,3,5}$ coordination mode, coordinating to one Tl each via one of the nitrile nitrogens (Tl–N = 2.60(4) Å) and the amide nitrogen (Tl–N = 2.90(3) Å), and to two Tl atoms via the other nitrile nitrogen (Tl−N = 2.79(4), 2.81(4) Å). Each octahedral Tl also coordinates (much more strongly) to two *trans* methyl ligands (Tl–C = 2.08(4), 2.15(5) Å). An unusual coordination mode ($\mu_{1,1,5,7}$) is also shown by tcm in the related Me$_2$Tl(tcm) compound, which again has a 3D network structure [128].

The second 3D M–dca network is that of [Cu(pn)$_2$][Mn(dca)$_4$], pn = 1,3-diaminopropane [114]. This structure contains zigzag Mn(dca)$_2$ chains in which each metal is bridged by double dca bridges. These chains are then interconnected by *cis* disposed *trans*-Cu(pn)(dca)$_2$ bridging moieties. This generates 3D diamond-related networks; three such networks interpenetrate. All dca ligands have the $\mu_{1,5}$ bridging mode, and only weak antiferromagnetic interactions are observed.

Three further compounds reported by Hvastijová et al. are worth noting, although no crystal structures have been determined. Cu(dca)$_2$(2-methylbenzimidazole)$_2$ is reported to be weakly antiferromagnetically coupled ($J = -0.4$ cm^{-1}) and to exhibit long-range antiferromagnetic ordering under ca. 15 K. No experimental evidence is presented to support this. IR analysis suggests $\mu_{1,5}$ bridging dca ligands [129]. Two polymorphs of Cu(dca)$_2$(imidazole) have been found to have different magnetic properties [130]. IR analysis suggests the α phase has $\mu_{1,5}$ bridging dca ligands ($J = -1.7$ cm^{-1}), while the β phase has $\mu_{1,3}$-dca ($J = -6.7$ cm^{-1}). Both compounds are postulated to show long-range magnetic ordering below 15.7 K, but this ordering is antiferromagnetic for the α phase and ferromagnetic for the β phase. Again, there is little evidence presented for this postulate.

3.4. Summary

In summary, we find that coligands are easily incorporated into M–dca networks, and the resultant structural modification results in a wide range of new networks with differing topologies. Unfortunately, magnetic exchange between metal centres in almost all the compounds discussed above is only very weak, if present at all, and antiferromagnetic in nature. This is, however, in keeping with the fact that all but a few structures contain only long $\mu_{1,5}$-dca bridges. Only one compound (Cu(dca)$_2$(1,10-phen)) with $\mu_{1,5}$-dca bridges showed possible ferromagnetic coupling. The two other sets of compounds discussed in this section that definitively show ferromagnetic interactions (i.e. the tube-like M(dca)$_2$(2-aminopyrimidine), and the 2D sheet-like M(dca)$_2$(H$_2$O) $\cdot$ phenazine), contain $\mu_{1,3,5}$-dca ligands. Long-range magnetic ordering is only observed in M(dca)$_2$(H$_2$O) $\cdot$ phenazine, M = Fe, Ni and Mn(dca)$_2$(H$_2$O)$_2 \cdot$ 2(2,5-Me$_2$pyz), even though the latter contains only $\mu_{1,5}$-dca bridges. This is, however, not unprecedented, β-Co(dca)$_2$ (vide supra), for example, has only $\mu_{1,5}$-dca and also shows long-range magnetic ordering [16,26].

Finally, although outside the scope of this review, there are a few unusual molecular structures involving dca worthy of consideration here. The syntheses of a triply bridged Fe(II) dimer, [LFe($\mu_{1,5}$-dca)$_3$FeL]BF$_4$, L = CH$_3$C(CH$_2$PPh$_2$)$_3$ and a tetrahedral tetramer containing both dca and cyanide bridges, [(LFe)$_3$($\mu_{1,5}$-dca)$_3$(CN)$_3$Fe(μ_1-dca)]BF$_4$, have been reported [131]. The three 'basal' Fe(II) ions are low-spin, while the apical Fe(II) is high-spin. No crystal structures of these compounds were determined, however, those of close $\mu_{1,5}$ RC(CN)$_2^-$ analogues were. The structure of [Cu(bpca)(H$_2$O)(dca)]$_2$, bpca = bis(2-pyridylcarbonyl)amidate was determined, and it was found that the metal ions were bridged into a dimeric arrangement by two $\mu_{1,3}$-dca ligands [70]. The Cu–N(amide) interaction, however, was weak (2.799(2) Å), and no intradimer magnetic interactions were observed. Co(dca)$_2$(2,2′-biimidazole)$_2$ is a rare example of monodentate μ_3-dca ligands coordinating (in a *trans* fashion) through only the amide nitrogen [132]. Hydrogen bonding interactions

between one of the nitrile nitrogens and the 2,2′-biimidazole chelates links the molecules into chains. However, the magnetic behaviour is that of a distorted mononuclear $^4T_{1g}$ cobalt(II) system. The compound $Fe(dca)_2(abpt)_2$, abpt = 4-amino-3,5-bis(pyridin-2-yl)-1,2,4-triazole was found to display spin crossover, $S = 2 \leftrightarrow S = 0$, which could be induced by both light and thermal activation [133]. The crystal structure showed that the iron is coordinated to two chelating ligands and two *trans* monodentate μ_1-dca ligands. Historically, this was the first mononuclear Fe(II)–dca complex to be discovered and the results were compared with the analogous $Fe(NCS)_2(abpt)_2$ compound. Our own, contemporaneous efforts led to high-spin complexes containing μ_1-dca ligands of type $Fe(dca)_2(4R\text{-}1,2,4\text{-triazole})_2(H_2O)_2$ which formed sheet-like hydrogen bonded arrays [134]. Very recently Real et al. have isolated dinuclear spin-crossover complexes of type $[Fe(N_5)(\mu_{1,5}\text{-dca})Fe(N_5)]^{3+}$, where N_5 is a pentadentate polypyridyl chelator [135].

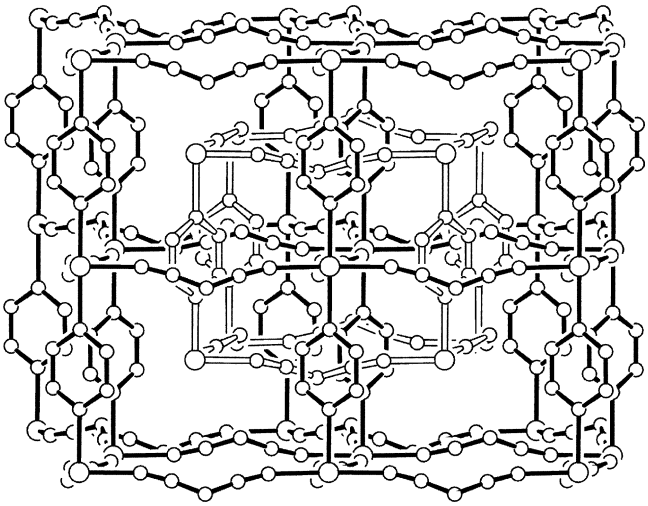

Fig. 14. Two interpenetrating 3D α-Po networks in the structure of α-$M(dca)_2$(pyrazine). Large circles represent the metal atoms.

4. Coordination polymers with bridging coligands

As well as the intense structural and topological interest in such mixed ligand species, it was hoped that introduction of a second bridging ligand would, in conjunction with dca bridging, yield enhanced magnetic coupling leading to long-range effects. The nature and length of the coligand will, of course, influence such magnetic effects. The long linker ligands such as 4,4′-bipyridine are expected to yield very weak coupling, but have been much used in designing network structures and microporous materials [2,3]. In fact, there are great advantages, in a wider crystal engineering context, in the use of dicyanamide and tricyanomethanide as a bridging ligands for coordination polymers. They are anionic, and thus networks formed with these ligands are unlikely to require anionic counterions to balance the charge of the metal atoms, as is the case for many other network compounds. Unlike other bridging anions such as the smaller pseudohalides (and with the exception of the large number of polycarboxylate donor ligands used [5f,5g,5h,5i,5j]), dca and tcm are also able to bridge reasonably large distances, and can act as three-connectors as well as two-connectors. Also, when acting as two-connectors the uncoordinated nitrogen atoms can accept hydrogen bonds from other components of the structure, which may stabilise or influence the networks formed.

4.1. Bidentate pyridyl-donor bridging coligands

Since the majority of bridging coligands used have been pyridyl donor ligands, we shall start with the simplest pyridyl-donor bridge of all, pyrazine. Two different topologies are formed with this ligand—3D nets (α) and 2D nets (β) [136–140]. The structures of α-$M(dca)_2$(pyrazine), M = Mn, Fe, Co, Ni, Cu, Zn are composed of two interpenetrating 3D networks with α-Po (or ReO_3) topology (Fig. 14). Each net is composed of 2D (4,4) sheets of metal atoms bridged by $\mu_{1,5}$-dca ligands that are then connected by the pyrazine ligands, generating the 3D networks [136,137]. The other polymorph, β-$M(dca)_2$(pyrazine), M = Co, Ni, Cu, Zn, consists of 2D (4,4) sheets (Fig. 15). In this polymorph, the $M(dca)_2$ substructure is composed of linear chains of metal atoms bridged by double $\mu_{1,5}$-dca bridges; these chains are then bridged by the pyrazine ligands to give a 2D (4,4) topology. Although the dimensionality and topology of the two polymorphs are vastly different, it is interesting to note that the local geometries of the metal ions are identical—four-equatorial $\mu_{1,5}$-dca bridges and two-axial pyrazine bridges. The different structures are a

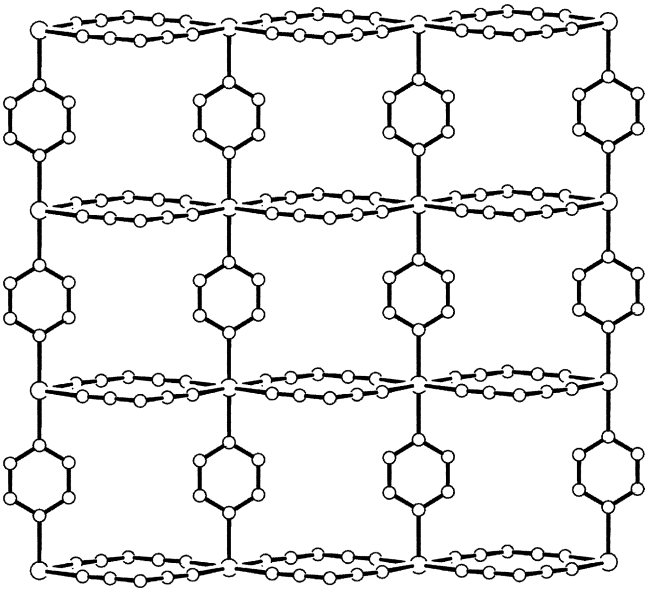

Fig. 15. The 2D (4,4) sheet structure of β-$M(dca)_2$(pyrazine). Large circles represent the metal atoms.

result of the different alternative $M(dca)_2$ substructures formed. Due to Jahn–Teller distortion, the Cu compounds have space groups different to the related structures with other metal ions (but the same Bravais lattice type and network topology) [136]. The α phase of the Cu compounds also appears to be metastable; if the green α phase is left to stand in the reaction mixture, it is transformed to the blue β phase after several days. No such transformation has been observed for the other metal complexes.

An interesting aspect of the α phase is that some of the compounds have been found to undergo phase changes. At 223 K and r.t., the Mn compound was found to be orthorhombic (space group *Pnma*), with the dca ligands showing disorder [137]. Structure determinations at 173 and 123 K, however, showed monoclinic ($P2_1/n$) symmetry and pseudo-merohedral twinning, with the dca ligands becoming ordered. Thus the disorder of the dca ligands at higher temperatures is dynamic since on lowering the temperature they become ordered in two possible orientations related by the twin law. This is also supported by an experiment conducted in which data were collected on a crystal below the phase change temperature, followed by heating of the crystal above the phase change (whereupon the dca ligands go from being ordered to disordered), then returning the crystal temperature to below the phase change (whereupon the dca ligands become ordered again) and collecting data again [137]. The proportions of each twin (i.e. the ratio between the two dca orientations) in the two data sets below the phase change were found to be different. The Fe compound was also found to display a similar phase change, although it occurs at a different temperature, at 173 and 223 K it was found to be $P2_1/n$ with pseudo-merohedral twinning, while at r.t. it was found to be *Pnma* with disordered dca ligands [137]. The pyrazine ligands were also disordered in the r.t. Fe structure.

Rotational motion of the pyrazine ligand in α-$Mn(dca)_2$(pyrazine) has been observed and studied in recent quasielastic neutron scattering experiments [140]. The motion involves a 180° rotational jump about the N···N axis of the ligand. Between 200 and 410 K the motion is on the scale of nanoseconds, while a phase change occurs at 408 K, and at 425 K this motion occurs on a time scale of picoseconds. Below 200 K the pyrazine is apparently static, but whether this change in the pyrazine rotational freedom is correlated with the structural switch between ordered and disordered dca ligands associated with the crystallographic phase change is, at present, unclear. β-$Cu(dca)_2$(pyrazine), which has a more compact structure, shows no rotational motion of the pyrazines.

The α- and β-$M(dca)_2$(pyrazine) series generally display weak antiferromagnetic coupling between high spin M(II) centres [136,137]. No changes in χ/T plots were evident at the temperature of the crystallographic phase changes, described above. Maxima in χ, at 3.5 K, were noted in the two Cu(II) isomers which allowed analysis using a 2D $S = 1/2$ Rushbrooke and Wood [141] model employing $g = 2.25$, $J = -2.6\ cm^{-1}$. α-$Fe(dca)_2$(pyrazine) has typical high spin d^6 Mössbauer parameters viz. $\delta = 1.20\ mm\ s^{-1}$, $\Delta E_Q = 2.36\ mm\ s^{-1}$ (4.2 K); compare α-$Fe(dca)_2$ $\delta = 1.21\ mm\ s^{-1}$, $\Delta E_Q = 3.17\ mm\ s^{-1}$ (77 K) and $Fe(dca)_2(H_2O)\cdot$phenazine, site 1: $\delta = 1.17\ mm\ s^{-1}$, $\Delta E_Q = 3.08\ mm\ s^{-1}$ (77 K), site 2: $\delta = 1.32\ mm\ s^{-1}$, $\Delta E_Q = 3.22\ mm\ s^{-1}$. It shows Curie–Weiss susceptibility and magnetic moment data indicative of orbital degeneracy ($^5T_{2g}$ parent), spin–orbit coupling and weak antiferromagnetic coupling; the latter confirmed by the linear dependence of magnetisation on field (0–5 T). This is quite unlike the susceptibility data noted for the ordered complexes α-$Fe(dca)_2$ and $Fe(dca)_2(H_2O)\cdot$phenazine because of the $\mu_{1,5}$-dca bridging mode and the Fe–pyrazine–Fe superexchange pathway. The Co(II) isomers tell a similar story and do not display the low temperature anomalies shown by the phenazine adduct and other Co(II)–dca and –tcm polymers. Only in the case of α-$Mn(dca)_2$(pyrazine) was long range order noted, of an antiferromagnetic type ($J = -0.12\ cm^{-1}$) with $T_N = 2.5$ K, and this was confirmed by neutron powder diffraction measurements [139]. Observation of a magnetic phase transition in only the Mn(II) member of the series probably relates to its high spin-multiplicity and lack of orbital degeneracy/spin–orbit effects. Linker ligands having shorter and more effective bridges than pyrazine would be required to get stronger net coupling, and consequent 3D order. Such was the case in some three-atom bridged pyrimidine complexes of Ni(II), Co(II) and Fe(II) [104,105], such as $Fe(\mu_{1,5}\text{-}dca)_2(pyrimidine)\cdot EtOH$ ($T_N = 3.2$ K) which is a canted-spin antiferromagnet [104], and the 2D compound $Fe(\mu_{1,5}\text{-}dca)_2(bpym)_{0.5}\cdot xH_2O$ which shows stronger short-range antiferromagnetic coupling than in $Fe(dca)_2$(pyrazine), viz. $J = -1.6\ cm^{-1}$, but no long-range order [142]. The Co(II)–bpym analogue showed antiferromagnetic coupling of similar magnitude. Clearly, the pyrimidine bridging pathway provides stronger coupling than does the $\mu_{1,5}$-dca pathway.

A derivative of pyrazine, 2,5-Me_2pyz, is contained in the structure of $Cu_2(dca)_4$(2,5-Me_2pyz) [143]. In this structure the metal atoms are five-coordinate, most likely due to the increased steric bulk of the ligand compared with pyrazine itself. The metal atoms are bridged by 2,5-Me_2pyz ligands and $\mu_{1,5}$-dca ligands into a rare five-connected 3D network; two such networks interpenetrate. A combination of χ versus T and M versus H data indicated that long-range antiferromagnetic order occurs, at $T_N = 5.0$ K, in this material.

Use of other sterically bulky derivatives of pyrazine, such as aminopyrazine, 2,5-Me_2pyz, Me_4pyz and phenazine, has resulted in structures with either monodentate or uncoordinated pyrazine derivatives; these were discussed in the previous section.

The pyrimidine ligand, mentioned earlier, is closely related to pyrazine, with the nitrogen atoms having a 1,3 disposition instead of a 1,4 disposition in the six-membered ring. As a result, the ligand bridges not in a linear fashion, but with a kinked 'V'-shaped geometry. The

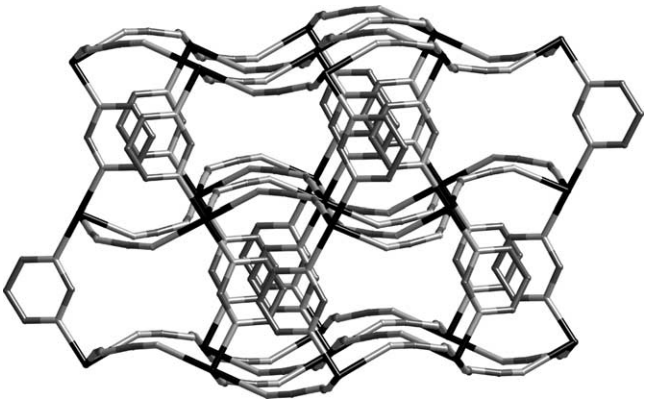

Fig. 16. The 3D network with distorted α-Po topology in the structures of $M(dca)_2(pyrimidine) \cdot solv$.

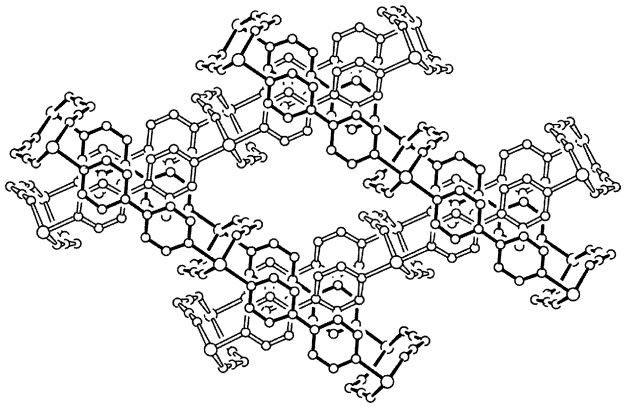

Fig. 17. The 2D inclined interpenetration of (4,4) sheets in the structure of $Co(dca)_2(4,4'\text{-bipy}) \cdot 1/2H_2O \cdot 1/2MeOH$. Large spheres represent metal atoms, and solvent molecules are omitted for clarity.

structures of $M(dca)_2(pyrimidine) \cdot EtOH$, M = Fe, Co, $Ni(dca)_2(pyrimidine) \cdot H_2O$ and $Cu(dca)_2(pyrimidine) \cdot MeCN$ are isomorphous [104,105,144]. The metal ions are bridged by $\mu_{1,5}$-dca ligands into (4,4) sheets, and then these sheets are bridged by the pyrimidine ligands to give 3D networks with α-Po topology (Fig. 16). The $M(dca)_2$ sheets are corrugated to accommodate the kinked nature of the pyrimidine bridge; this and the shorter M···M distance across this bridge means that, unlike the analogous pyrazine compounds, solvent molecules are included in the structure rather than a second interpenetrating network. No significant magnetic coupling is observed for the Cu compound, however, as indicated above, the Fe, Co and Ni complexes show spontaneous magnetisation below transition temperatures of 3.2, 1.8 and 8.3 K, respectively.

The 4,4′-bipyridine (4,4′-bipy) ligand, like pyrazine, is a linear pyridyl-donor bridging ligand, but is considerably longer and generates a much more varied array of structures [106,107,145]. We have already discussed the tube-like structures formed with monodentate 4,4′-bipy ligands, and we will discuss here structures with bridging 4,4′-bipy coligands. A much wider variety of structures has been discovered compared with those containing the pyrazine ligand.

The structures of $M(dca)_2(4,4'\text{-bipy})$, M = Fe, Co, Ni [106,107,145] all contain interpenetrating α-Po 3D networks. Metal ions are bridged by *trans* 4,4′-bipy and $\mu_{1,5}$-dca ligands, and despite the longer length of the coligand length, they, like the pyrazine α phase compounds, contain only two interpenetrating nets. The structure of $Co(dca)_2(4,4'\text{-bipy}) \cdot 1/2H_2O \cdot 1/2MeOH$ [106] also contains bridging 4,4′-bipy and $\mu_{1,5}$-dca ligands, however, it displays 2D (4,4) sheet topology, analogous to the β phase of the pyrazine derivatives. Linear $M(dca)_2$ chains containing double dca bridges are crosslinked by *trans* 4,4′-bipy ligands to generate the sheets. The larger length of the 4,4′-bipy bridge means that, unlike the pyrazine derivatives, this compound displays inclined interpenetration (Fig. 17). The structure of $Cu(dca)_2(4,4'\text{-bipy}) \cdot H_2O$ also has 2D (4,4) nets showing inclined interpenetration [106]. In this structure, however, the 4,4′-bipy ligands bridge between linear M(dca) chains formed by single $\mu_{1,5}$-dca ligands bridging between the metal atoms. The five-coordinate copper atoms are also bound to monodentate μ_1-dca ligands. These monodentate dca ligands, however, also form weaker interactions between their amide nitrogens and the copper atoms (Cu–N = 2.867 Å). These interactions cross-link the interpenetrating sheets into a single 3D network, and give the copper atoms pseudo-octahedral geometries and the dca ligands involved a pseudo-$\mu_{1,3}$ bridging mode.

The structures of $Cu(dca)_2(4,4'\text{-bipy}) \cdot S$, $S = H_2O$, MeOH are isomorphous and contain 2D (4,4) sheets with the same topology as the previous compound [106]. In these structures, however, the Cu(dca) chain substructure has a zigzag geometry, and interpenetration of networks does not occur. The Cu ions again have a weak sixth interaction, this time to solvent molecules (Cu–O = 2.925(3), 2.917(2) Å, respectively).

Finally, two 4,4′-bipy structures have been reported with only monodentate dca ligands. $Fe(dca)_2(4,4'\text{-bipy})(H_2O)_2 \cdot 4,4'\text{-bipy}$ [106] consists of linear chains of metal ions bridged by *trans* 4,4′-bipy ligands. The coordination spheres of the Fe atoms are completed by two *trans* water ligands and two *trans* μ_1-dca ligands. The structure also includes uncoordinated 4,4′-bipy molecules. Hydrogen bonding interactions between the uncoordinated 4,4′-bipy molecules and the water ligands, and between the uncoordinated nitrile nitrogens of the monodentate dca ligands and the water ligands link the chains into two interpenetrating α-Po 3D networks. The structure of $Zn_3(OAc)_4(4,4'\text{-bipy})_3(dca)_2$ contains 1D polymers with an unusual 'three-legged ladder' topology [146]. The rungs of the ladders each contain three Zn atoms bridged by four acetate ligands; these rungs are linked by triple 4,4′-bipy bridges. The monodentate μ_1-dca ligands are coordinated to the sides of these ladders.

As expected from the large M–4,4′-bipy–M separations, and the poor superexchange properties of 4,4′-bipy, the magnetic properties of the various high-spin $M(dca)_2$–4,4′-bipy phases are generally indicative of very weak to zero

antiferromagnetic coupling and a consequent absence of long-range order. The $\mu_{1,5}$-dca bridges cannot compensate for the 4,4′-bipy bridges in the way that chloride bridging can in $CoCl_2$(4,4′-bipy), which displays metamagnetic ordering, $T_N = 5.0$ K [147], and $\mu_{1,3}$-azido bridging can in $Mn(N_3)_2$(4,4′-bipy), which displays a canted-spin ground state, $T_N = 42.5$ K [148].

The ligand 1,4-bis(4-pyridyl)ethane (bpea) is a longer, more flexible analogue of 4,4′-bipy. Two isomorphous structures have been reported with this coligand. The structures of M(dca)$_2$(bpea), M = Mn [108], Cu [72] contain 1D chains in which each pair of adjoining metals is triply-bridged by two $\mu_{1,5}$-dca ligands and one bridging 'U'-shaped bpea ligand. The bpea ligands coordinate in a *trans* fashion to the metal ions, with dca ligands occupying the other four-coordination sites. Weak intrachain antiferromagnetic interactions are observed for both compounds ($J = -1.25$ and -0.22 cm^{-1}, respectively).

The even longer bridge 1,3-bis(4-pyridyl)propane (bpp) has been found to form two polymorphs with the formula Cd(dca)$_2$(bpp) [149]. One polymorph has a 1D chain structure analogous to the bpe structures described above, while the second polymorph has a 2D sheet structure. The sheets contain 1D zigzag M(dca)$_2$ chains in which adjacent metal ions are bridged by double $\mu_{1,5}$-dca bridges. The bpp ligands coordinate in a *cis* fashion, and connect the chains into 2D sheets with (4,4) topology. These sheets are highly corrugated, and show very unusual 2D→3D parallel interpenetration [3].

A rich variety of structures has been obtained from the reaction of Cu(I), dca and various pyridyl-donor bridging ligands [117]. The structure of Cu(dca)(Me$_4$pyz)$_{1/2}$ is composed of 2D (6,3) sheets in which trigonal Cu(I) ions are bridged by Me$_4$pyz and $\mu_{1,5}$-dca ligands. Reaction of Cu(I) and dca with 4,4′-bipy results in two products—a kinetic product, in the form of yellow–orange dichroic crystals, and a thermodynamic phase, which forms as dark red crystals after 1–3 days at the expense of the kinetic phase. The initial product, Cu$_2$(dca)$_2$(4,4′-bipy)(MeCN)$_2 \cdot$ 1/2(4,4′-bipy), is composed of 1D ladder-like polymers. The sides of the ladders are formed by tetrahedral copper atoms bridged by single $\mu_{1,5}$-dca bridges, while the rungs are formed by bridging 4,4′-bipy ligands. The tetrahedral coordination spheres of the copper atoms are completed by terminal acetonitrile ligands, while uncoordinated 4,4′-bipy molecules are included in square channels formed by the packing of the ladders. The final product, Cu$_4$(dca)$_4$(4,4′-bipy)$_3$(MeCN)$_2$, is composed of thick 2D layers in which the metal ions are bridged by both 4,4′-bipy and $\mu_{1,5}$-dca ligands. These layers interpenetrate in an unusual 2D→3D parallel interpenetration mode [3]. Interestingly, the ratio of acetonitrile is the only difference in the formulae of these two compounds.

The analogous reaction with 1,4-bis(4-pyridyl)ethene (bpee) also produces two products, however, in this case they both appear to be thermodynamically stable and have the same formula, Cu(dca)(bpee). The structure of the α-Cu(dca)(bpee) polymorph consists of 2D (4,4) sheets showing twofold 2D→2D parallel interpenetration [3] in which the metal ions are bridged by both bpee and $\mu_{1,5}$-dca ligands. The same ligands bridge in the β polymorph, however, this structure contains five interpenetrating 3D diamondoid networks that exhibit a very unusual interpenetration topology.

An interesting series of structures has also been obtained through reaction of Cu(I), tcm and three different bridging ligands [150]. The networks all display 2D (4,4) sheet topologies, but different modes of maximising packing efficiency (interdigitation, interpenetration, intercalation). Cu(tcm)(hmt), hmt = hexamethylenetetramine contains interdigitating sheets, Cu(tcm)(4,4′-bipy) shows twofold 2D→2D parallel interpenetration, while Cu(tcm)(bpee) $\cdot$ 1/4bpee $\cdot$ 1/2MeCN shows intercalation of molecular species into channels created by the sheet packing. Significantly, the 4,4′-bipy and bpee structures differ significantly from the analogous dca structures, even though the tcm ligands all have a bidentate $\mu_{1,5}$ bridging mode (as do the dca analogues).

Reaction of Ag(tcm) with various bridging ligands results in a number of interesting coordination polymers [57,58]. The structures of Ag(tcm)(L)$_{1/2}$, L = pyrazine, 4,4′-bipyridine, 1,4-diazobicyclo-[2.2.2]-octane have the same network topologies. The silver atoms are bridged by tridentate tcm anions into (6,3) nets, and these sheets are linked together by the linear bridging coligands. Thus each silver atom is five-coordinate, and in these structures two such 3D nets interpenetrate. The 3D networks in Ag(tcm)(hmt) have the same topology, however, in this structure the hmt ligands are three-connecting, the tcm anions are two-connecting, and there is no interpenetration. The structure of Ag(tcm)(phenazine)$_{1/2}$ has two interpenetrating 3D networks constructed by the bridging of layers of doubly interpenetrating 2D (6,3) sheets of Ag(tcm) (similar to those in the structure of Ag(tcm) itself (vide supra)) by phenazine ligands.

Ag(tcm)(methylpyrazine)$_{3/2}$ contains ladder-like 1D polymers in which Ag($\mu_{1,5}$-tcm) chains form the sides and bridging methylpyrazine ligands the rungs. The tetrahedral silver atoms are also coordinated to monodentate methylpyrazine ligands. The structure of Ag(tcm)(bpee), bpee = 1,4-bis(4-pyridyl)ethene also contains ladder-like motifs, however, in this case the rungs are defined by bridging bidentate tcm anions and Ag(bpe) chains define the sides. 'Uncoordinated' tcm anions are also present, and weaker secondary interactions between both the silver atoms and both types of tcm anions define two interpenetrating 3D networks. Finally, the structure of Ag(tcm)(Me$_4$pyz)$_{1/2}$, Me$_4$pyz = tetramethylpyrazine contains 2D networks in which tube-like Ag(tcm) 1D nets are linked by bridging Me$_4$pyz ligands. The 'tubes' are composed of two Ag(tcm) chains in which the silver atoms are bridged by two-coordinate tcm anions. The two adjacent chains are then connected to each other via significantly longer bonds

from the tcm nitrogen atoms not involved in the intrachain bonding to the silver atoms of the other chain. These nitrogen atoms bond to the silver atoms with a rather low CN–Ag angle of 101.6(1)°.

4.2. Other bridging coligands

Nicotinic acid (Hnic, 3-pyridylcarboxylic acid) contains both a pyridyl donor group and a carboxylic acid donor group. In the structure of $Co_3(dca)_2(nic)_4(H_2O)_8 \cdot 2H_2O$, ladder-like 1D nets are formed in which the nic anion acts as both a monodentate ligand, coordinating via the pyridyl nitrogen, and a bridging ligand, coordinating via both the pyridyl nitrogen and a carboxylate oxygen atom [151]. The ladders are constructed from $Co(nic)(H_2O)_2$ moieties bridged into linear chains by $\mu_{1,5}$-dca ligands that coordinate to the metal ions in a *cis* fashion. These chains form the sides of the ladders; the rungs of the ladders are formed by $Co(H_2O)_4(nic)_2$ bridges. Only very minimal magnetic coupling between metal centres is observed.

The isomorphous structures of $M(dca)_2(apo)$, M = Co, Ni, Mn, apo = 2-aminopyridine *N*-oxide, contain complicated 3D networks [152]. $M_2(apo)_2$ dimers, in which the metal atoms are bridged by the apo oxygen atoms, are bridged in a helical fashion by $\mu_{1,5}$-dca ligands; each dimer is connected via these bridges to eight other dimers. The susceptibilities were analysed using a two-*J* model in which *J* is the intradimer constant and *J*′ is the interdimer constant. Maxima in χ_M versus *T* plots were indicative of antiferromagnetic coupling. Best-fits yielded $J = -17.8$ cm^{-1}, $J' = 2.7$ cm^{-1} (Co); $J = -40$ cm^{-1}, $J' = 1.5$ cm^{-1} (Ni); $J = -1.3$ cm^{-1}, $J' = -0.18$ cm^{-1} (Mn).

The structure of [Cd(tcm)(hmt)(H_2O)](tcm), hmt = hexamethylenetetramine has a complicated 3D network which can be related to the rutile network [153]. The Cd ions are connected by tridentate tcm anions and hmt ligands which coordinate to two Cd centres and hydrogen bond to a water ligand coordinated to a third. In addition, the structure contains uncoordinated tcm anions which also hydrogen bond to the water ligands. Bridging $B(OMe)_4^-$ and $\mu_{1,5,7}$ tcm anions connect seven-coordinate Cd ions into a chiral 3D network in the structure of $Cd(tcm)(B(OMe)_4) \cdot x$MeOH [154].

In the previous section we described a few structures that contain terminal 2,2′-bipyrimidine (bpym) coligands. The bpym ligand, however, can also act as a bridging ligand, and three different structural types have been reported to date which contain this ligand and dca. The structures of $M_2(bpym)(dca)_4 \cdot H_2O$, M = Fe [142], Co [65], Ni [155] contain 2D (4,4) sheets (Fig. 18). The metal ions are linked in one direction by single $\mu_{1,5}$-dca bridges, and in the other by alternating bpym and double $\mu_{1,5}$-dca bridges. The structures of $M_2(bpym)(dca)_4$, M = Mn [67], Cu [67,70], Zn [155] have 3D networks based on 1D ladders in which bridging bpym ligands provide the rungs and the sides are defined by metal ions bridged by *trans* disposed single $\mu_{1,5}$-dca bridges. These ladders are then cross-linked into 3D networks by further *cis* disposed $\mu_{1,5}$-dca bridges. The third structure type, 2D (6,3) sheets, is formed by $Fe_2(bpym)(dca)_4(H_2O)_2$ [142]. Each Fe centre is connected to three others by one bpym bridge and two $\mu_{1,5}$-dca bridges. The coordination spheres of the Fe atoms are completed by terminal water and μ_1-dca ligands. Hydrogen bonding interactions between the water ligands and the uncoordinated nitrile nitrogen atoms of the monodentate dca ligands connected these sheets into a 3D net. In all structures described here the magnetism is dominated by coupling across the bpym bridge, with any contribution via the $\mu_{1,5}$-dca bridges being negligible.

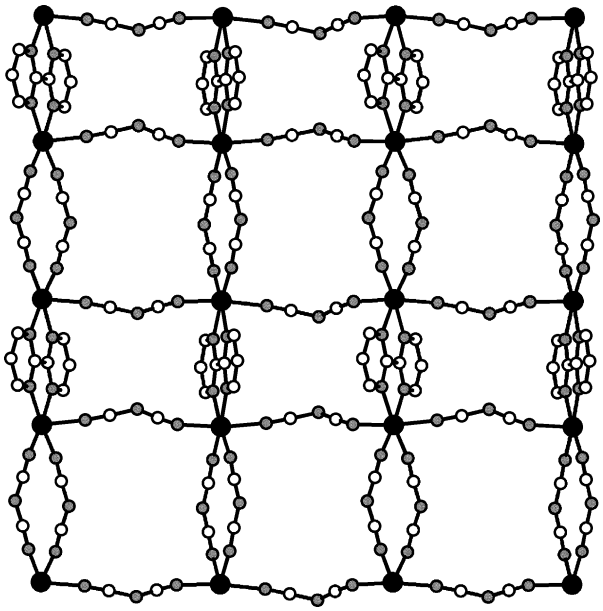

Fig. 18. The 2D (4,4) sheet structure contained in $M_2(bpym)(dca)_4 \cdot H_2O$. Atom shading as for Fig. 1. Water molecules are omitted for clarity.

The ligand HAT (1,4,5,8,9,12-hexaazatriphenylene) generates an unusual 3D network structure, $Co_3(HAT)(dca)_6(H_2O)_2$ [156]. Although the porous nature of this compound results in a poorly resolved structure, the network is formed by bridging $\mu_{1,5}$-dca ligands and tris-bidentate HAT ligands. The network can be described in terms of $Co_4(HAT)(dca)_3$ tetrahedral cages. The metal ions occupy the corners of a tetrahedron, the HAT ligand covers one face of the tetrahedron, and the dca bridges connect the three Co ions coordinated to the HAT ligand to the Co ion occupying the fourth corner of the tetrahedron. These tetrahedra are connected together by $\mu_{1,5}$-dca ligands and shared Co ions, such that each tetrahedron is connected to six others in a 3D network with α-Po topology (taking the tetrahedral cages as nodes). The compound also contains uncoordinated dca anions, however, the non-framework portion of the structure is poorly resolved and these were not identified crystallographically. The χT versus *T* data were characteristic of uncoupled Co(II) centres and fitted well to a zero-field split $S = 3/2$ model with $g = 2.01$ and $D = 38.9$ cm^{-1}. There was no evidence for any long-range ordering. The net effect of HAT and $\mu_{1,5}$-dca bridging is to yield extremely weak short-range coupling.

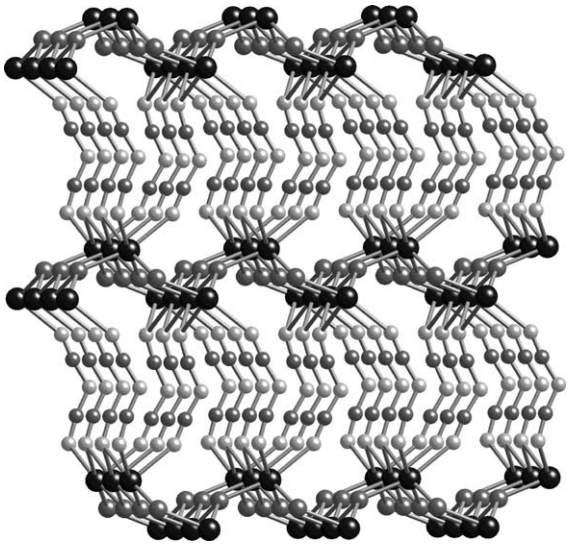

Fig. 19. The structure of Cd(OH)(dca). Cd atoms are shown as large black spheres, oxygen atoms as large grey spheres, carbon atoms as small grey spheres, and nitrogen atoms as small pale spheres.

As briefly mentioned earlier, Kurmoo [126,127,157] has reported two metal hydroxide based materials which contain dca and tcm, namely $Co_5(OH)_8X_2 \cdot 6H_2O$ and $M_2(OH)_3(dca)_2$, X = dca, tcm, M = Ni, Cu. The Co and Ni compounds were found to show long-range magnetic ordering—ferrimagnetic for Co ($T_c = 58$ K (dca), 38 K (tcm)), ferromagnetic for Ni ($T_c = 25$ K (dca), 23 K (tcm)). The copper compounds show no long-range ordering. Detailed structural data, however, have not been reported, although the compounds are thought to contain metal hydroxide layers separated by dicyanamide molecules. In the case of the Co complex, IR analysis has indicated monodentate μ_1-dca ligands.

Recently, however, we have determined the structure of Cd(OH)(dca), synthesised inadvertently from an aqueous methanolic reaction containing Cd(II), dca and tetramethylpyrazine [158]. Although the latter does not appear in the product, it presumably acts as the hydroxide-generating base in this reaction. The structure, shown in Fig. 19, consists of Cd(OH) layers bridged by dca ligands showing an unprecedented $\mu_{1,1,5}$ bridging mode. The monodentate nitrile nitrogen also forms a hydrogen bonding interaction with the tridentate hydroxide ligand.

4.3. Summary

Both dca and tcm form a wide variety of 1D, 2D and 3D network structures when combined with bridging coligands. The fact that the dca and tcm ligands act not only as bridges but also as counterions means that interpenetration is commonly observed; uncoordinated counterions, which often lie in the network cavities and block interpenetration, are not required. Polymorphism also seems to be a particularly common occurrence in these systems. For example, two polymorphs are formed when dca and pyrazine ligands are combined, while even greater numbers of structural types have been discovered for the dca–4,4′-bipy combination. The pyrazine compounds also display complex crystallographic twinning, and phase changes are prevalent. Not suprisingly, increasing the steric bulk of pyrazine-type coligands in the M–dca systems decreases the coordination modes of these ligands from bidentate to monodentate to uncoordinated.

Apart from the structure of Cd(OH)(dca), the bridging dca ligands in all the structures with bridging coligands adopt the $\mu_{1,5}$ coordination mode. For tcm, however, the tridentate bridging mode is more common. This means that magnetic exchange in these materials is generally very weak, except where the bridging coligands themselves are good propagators of magnetic exchange (i.e. bipym, pyrimidine, apo, hydroxide). The compounds α-$Mn(dca)_2$(pyrazine) and $Cu_2(dca)_2$(2,5-Me_2pyz) do show long-range ordering, but only at very low temperatures ($T_N = 2.5$ [138,139] and 5.0 K [143], respectively).

5. Cation templation of anionic metal–dca networks

We have described in the previous two sections how the introduction of coligands can be used to modify the topology of metal dicyanamide networks. Another very effective approach, however, is to synthesise anionic metal dicyanamide networks. These anionic networks require the presence of countercations; variation of the size, shape and charge of these countercations can be used to vary the topology of the anionic networks.

For example, consider the isomorphous structures of $(Ph_4E)Mn(dca)_3$, E = P, As [159,160]. The anionic $Mn(dca)_3^-$ nets have 2D (4,4) topology in which metal ions are bridged in one direction by single $\mu_{1,5}$-dca bridges, and in the other by double $\mu_{1,5}$-dca bridges (Fig. 20). These

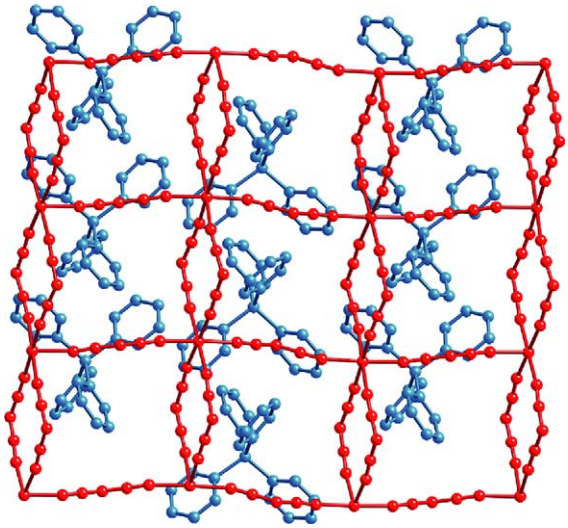

Fig. 20. The structure of $(Ph_4E)M(dca)_3$, with the 2D (4,4) anionic network (red) in the foreground, and the cation packing (blue) in the background.

anionic sheets alternate with layers of Ph_4E^+ cations that show distinct intercation supramolecular interactions. The cations form columns in which adjacent cations show orthogonal fourfold phenyl embraces (O4PEs) [161]. The columns are interconnected by intercation $\pi\cdots\pi$ interactions.

These intercation supramolecular interactions are easily disrupted by replacement of one or more phenyl groups of the cation with alkyl substituents. Thus use of $MePh_3P^+$ countercations produces a 3D network (Fig. 21). The anionic networks in $(MePh_3P)Mn(dca)_3$ are composed of metal ions bridged by both single and double $\mu_{1,5}$-dca ligands and possess a novel five-connected topology [159]. The cations lie in pairs in cavities within the network (Fig. 21) and exhibit pseudo-sixfold phenyl embrace (pseudo-6PE) intercation interactions [162].

While the network topologies are different, all three of these Mn structures display similar magnetic properties, indicative of weak antiferromagnetic coupling.

The structures of $(Ph_4P)Co(dca)_3$ [160,163] and $(Ph_4As)M(dca)_3$, M = Co, Ni [164] have the same 2D (4,4) sheet structure as the Mn derivatives, although the single $\mu_{1,5}$-dca bridges are disordered in some of the structures and ordered in others (with a resultant doubling of one unit cell length). The μ_{Co}/T data for $(Ph_4As)Co(dca)_3$ are indicative of $^4T_{1g}$ temperature dependent behaviour, with the unusual field dependence in μ_{Co} evident below 20 K such that a minimum is noted, at 9 K, in fields of 0.01 and 0.1 T but not in fields of 1 or 2 T. Similar behaviour was displayed by the 3D $MePh_3P^+$ salt. Such behaviour for Co(II) has been mentioned earlier and probably originates from Zeeman splitting combined with weak exchange coupling. DC and AC susceptibility tests for long-range order proved negative. This was not the case, however, for $(Ph_4As)Ni(dca)_3$, which ordered below 20.1 K [164]. We took great care, using AC data and hysteresis loops, to show that this transition was not due to contaminating α-$Ni(dca)_2$. The Ph_4P^+ salt also showed order, but, surprisingly, the 3D $MePh_3P^+$ salt did not. These differences remain intriguing. 2D sheet systems are generally not expected to show long-range order but there are many examples now known which do, including some discussed herein [126,127,165].

Solvated species can also be obtained from the cation templation reactions described above. In particular, the structures of $(Ph_4As)_2[M_2(dca)_6(H_2O)]\cdot H_2O\cdot x$MeOH, M = Co ($x = 1$), Ni ($x = 0.5$) [164] contain 1D ladder-like networks. The ladders contain linear chains of metal ions bridged by double $\mu_{1,5}$-dca bridges. These chains are linked in pairs by single $\mu_{1,5}$-dca ligands to generate the ladder motif. The peripheries of the ladders contain monodentate μ_1-dca ligands and water ligands; hydrogen bonding interactions between these ligands and intercalated water and methanol molecules link the ladders into 2D layers. These layers alternate with layers of Ph_4As^+ cations that again exhibit extensive intercation supramolecular interactions. Like the $(Ph_4E)M(dca)_3$ structures, columns of cations showing O4PE interactions are present. In this case, however, the columns are linked together by both $\pi\cdots\pi$ and C–H$\cdots\pi$ interactions. Magnetic studies on these methanolate species demonstrated the great care needed to eliminate traces of the ferromagnets α-$M(dca)_2$, M = Co, Ni evident at 9.0 and 21.0 K. The μ/T plot for Co is similar to that for the $Co(dca)_3^-$ phase.

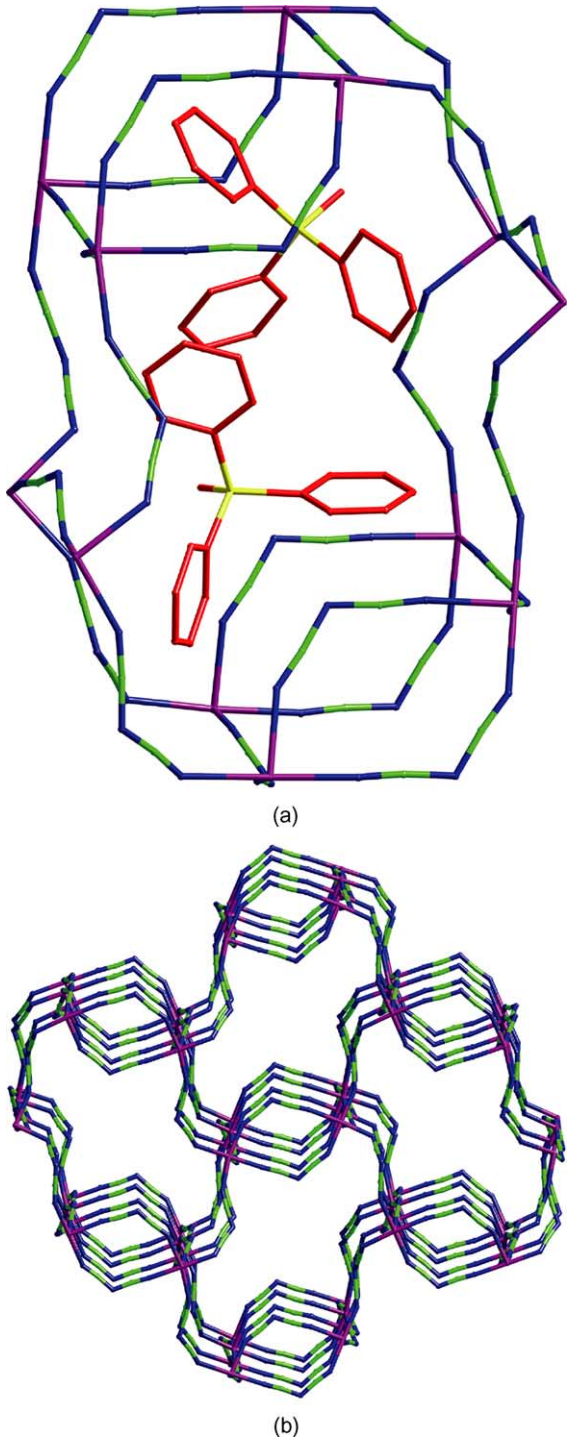

Fig. 21. The structure of $(MePh_3P)Mn(dca)_3$, showing (top) two cations within a single network cavity, and (bottom) the overall 3D network of the anion (cations omitted for clarity).

Exposure of the Ni solvate to air leads to loss of methanol and appearance of magnetically ordered behaviour. In contrast, fresh samples sealed in a quartz tube showed no magnetic order.

An anionic $M(dca)_4^{2-}$ network has also been reported. The structure of $(Ph_4P)_2Co(dca)_4$ contains 1D linear chains in which metal atoms are connected by double $\mu_{1,5}$-dca bridges [160,163,166]. The octahedral metal coordination geometries are completed by *trans* monodentate μ_1-dca ligands. Magnetic data indicate very weak coupling, a minimum in the μ/T plot of the type discussed for $(Ph_4As)Co(dca)_3$ being assigned by one group [166] to ferromagnetic coupling, with ferromagnetic order below 1.75 K. This needs confirmation.

The use of the metal-containing $M(2,2'\text{-bipy})_3^{2+}$ cations, some of which are paramagnetic, produces the compounds $[M(2,2'\text{-bipy})_3][M'(dca)_3]_2$ ($M = Fe$, $M' = Mn$ or Fe; $M = Ni$, $M' = Mn$) [167]. These compounds contain 2D (6,3) $M(dca)_3^-$ sheets (Fig. 22) in which each metal ion is connected to three others by three pairs of $\mu_{1,5}$-dca ligands. The cations lie within the hexagonal windows of the anionic sheets. The magnetic susceptibilities are summations of those from the cationic and anionic contributions and no sub-lattice interactions are evident to date. Other mixed metal compounds of type $[Cu(en)_2][Mn(dca)_4]$ have been described above. We are continuing work with cations of various structural and magnetic types in order to produce hybrid species along the lines used in metal–oxalate anionic networks [10,11]. Many novel structural types are emerging.

The use of the bis(ethylenedithio)tetrathiafulvalene) (ET) radical cation generates a number of anionic Cu(I) coordination polymer materials that display very interesting magnetic and electrical properties. The compounds κ-$(ET)_2Cu(dca)X$, $X = Br$, Cl are isomorphous, with the chloride and bromide materials being superconductors ($T_c = 12.5$, 11.6 K, respectively) [168]. The coordination polymer consists of 1D chains of trigonal Cu(I) ions bridged by $\mu_{1,5}$-dca ligands and coordinated to terminal halide ions. The origin of the superconductivity, however, lies in the packing arrangement of the layers of ET radical cations. Two structures with cyanide coligands and vastly different properties have also been reported. θ-$(ET)_2Cu(dca)_2(CN)$ is a two-dimensional Heisenberg antiferromagnet below ca. 220 K and shows no superconductivity [169]. The coordination polymer substructure consists of (6,3) sheets of trigonal cuprous ions bridged by cyanide and $\mu_{1,5}$-dca ligands, with layers of doubly interpenetrating sheets formed. κ-$(ET)_2Cu(dca)(CN)$, however, is a superconductor with a T_c of 11.2 K [170]. The coordination polymer substructure consists of trigonal Cu(I) ions bridged by cyanide ligands into zigzag chains; the dca ligands coordinate in a mondentate μ_1 fashion.

Finally, two Cu–dca polymers have been reported which might be considered to be cation-templated, although the cations are coordinated to the networks [171]. The structure $[Tl(18\text{-crown-}6)][Cu(dca)_2]$ contains 2D (4,4) sheets of Cu(I) ions bridged by $\mu_{1,5}$-dca ligands; half these ligands also coordinate to the Tl atoms via their amide nitrogen atoms. The structure of $[Rb(18\text{-crown-}6)]_3[Cu_2(dca)_5]$ contains highly branched 1D $Cu_2(dca)_5^{3-}$ networks containing both 'bridging $\mu_{1,5}$' and 'monodentate μ_1' dca ligands. These 1D nets are connected into an overall 3D net by interactions between the Rb cations and both the nitrile nitrogens of the 'monodentate' ligands (giving a final $\mu_{1,5}$ bridging mode) and amide nitrogen atoms of half of the $\mu_{1,5}$-dca ligands (generating a final $\mu_{1,3,5}$ bridging mode). The related non-polymeric structure of $[Cs(18\text{-crown-}6)](dca)\cdot H_2O$ has also been reported [172].

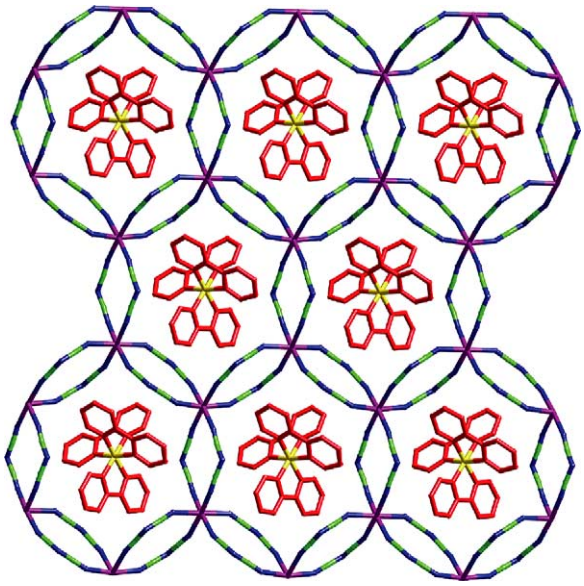

Fig. 22. The 2D (6,3) topology observed in the structures of $[M(2,2'\text{-bipy})_3][M'(dca)_3]_2$.

6. Concluding remarks

We have presented an up-to-date and detailed review of the structural and magnetic features of coordination polymers containing dicyanamide and/or tricyanomethanide bridging ligands. These anionic pseudohalide ligands have been shown to be excellent ligands for the formation of network structures. In particular, M–dca networks are particularly 'malleable' [2a], with modification of the $M(dca)_n$ substructure topology readily achieved through introduction of coligands or by cation templation. The ability of systems like the M–dca networks to adopt a variety of network topologies and ligand bridging modes allows the relationship between crystal structure and physical properties to be explored over a wide range of related systems. In this way, useful data on the relative importance of various structural features in particular materials can be determined, and new 'designs' which optimise particular physical properties can be delineated. The relationship observed to date between structure and magnetic properties in dca- and tcm- containing coordination polymers is summarised below.

The structural types range from the binary rutile-like networks α-M(dca)$_2$ and M(tcm)$_2$, through the self-penetrated M(dca)(tcm), to an array of interpenetrated and interdigitated ternary structures in the species M(dca)$_2$L$_n$, where L is a terminal or bridging Lewis-base donor ligand. The anionic M(dca)$_3^-$ and M(dca)$_4^{2-}$ networks display 2D or 3D structures dependent upon the nature of the templating cation; often only subtle changes in cation characteristics are required for substantial change in anionic network topology to occur.

Polymorphism and the formation of multiple products in a single reaction mixture are particularly common in dca chemistry, and particular care should always be taken when examining new materials. Reactions should always be closely scrutinised for formation of multiple products, and characterisation of bulk products by powder diffraction is very important, especially when materials show interesting magnetic properties. On more than one occasion we have been initially misled by a magnetically ordered minor product.

From a magnetic point of view, the long-range ordered materials α-M(dca)$_2$ have caused great interest in the context of homometallic molecular magnets, and complement extensive studies made in recent years on μ-cyano (Prussian blue), μ-oxalato and μ-oxamido heterometallic compounds. Whereas the nearest neighbour exchange coupling in the latter systems have been primarily influenced by the nature of the 'magnetic' d-orbital on each metal, leading, for instance, to orthogonal overlap, and ferromagnetic coupling in appropriate cases (e.g. J_{t_{2g}/e_g} contributions in M–CN–M′ systems), the structural features in homometallic extended framework magnets of the dca type, or of halide- [173], imidazolate- [174] or organophosphate- [173,175] bridged systems, also play a major role. We believe that we have uncovered large parts of the 'M–dca iceberg', the tip of which was recently highlighted by Day [176].

The α-M(dca)$_2$ compounds have been subjected to a battery of modern solid state physics techniques (e.g. muon rotation studies, neutron diffraction) in order to discover their innermost magnetic secrets. The results of these measurements have been reviewed here, together with descriptions of calculations of superexchange used to understand the different types of ground state coupling, ranging from antiferromagnetic (Cr, Mn, Fe) to ferromagnetic (Co, Ni, and, possibly, Cu). The $\mu_{1,3}$-dca bridging pathway yields the lowest J value in both a Goodenough-type superexchange model for the rutile network and in density functional theory calculations. As the number of holes in the t_{2g}^6 levels in the M(II) ion increase, so does the antiferromagnetic character increase, thus leading to order of the canted-spin antiferromagnetic type in M = Cr, Mn, Fe.

In the ternary species involving terminal or bridging Lewis-base donors, it was hoped, at the outset, that magnetostructural correlations (e.g. of the type well established for dinuclear μ-dihydroxycopper(II) cluster compounds [177]) would be obtained from the many 1D and higher dimensionality structures now available, most of which contain $\mu_{1,5}$-dca bridges. Unfortunately the spread of J values is too small to make correlations with e.g. M···M distance or dca geometry, the majority of these J values being negative and less than one wavenumber, even in cases where a second bridging ligand (e.g. pyrazine, 4,4′-bipyridine, pyrimidine) is present. Reasons for the very weak coupling occurring across $\mu_{1,5}$-dca bridges, compared, say, to $\mu_{1,3}$ azide bridging, have been given in terms of ligand-to-metal 'magnetic' orbital overlap concepts [89].

While the correlation between $\mu_{1,3}$-dca bridging and stronger coupling/long-range order holds in many cases, it is not infallible. Examples such as β-Co($\mu_{1,5}$-dca)$_2$, Mn($\mu_{1,5}$-dca)$_2$(pyrazine), M($\mu_{1,5}$-dca)$_2$(pyrimidine) and (Ph$_4$As)[Ni($\mu_{1,5}$-dca)$_3$] break such a prediction. The availability of very low temperature instrumentation such as neutron diffraction has also revealed long-range order in tcm species having $\mu_{1,5}$ bridging modes such as Mn(tcm)$_2$ [50].

To date, the anionic networks of type M(dca)$_3^-$ do not reveal any magnetic interactions occurring between the anionic sublattice and magnetic cation sublattices (e.g. M(2,2′-bipy)$_3^{2+}$).

From a general perspective, the dca and tcm coordination polymers have yielded much valuable fundamental information on homometallic magnets, albeit at ordering temperatures below 50 K. The poor superexchange capabilities of these diamagnetic cyano-based bridging groups means that ordering temperatures close to r.t. are unlikely to be attained, unless, for instance, new materials containing coligands of the μ-cyano or μ-hydroxide (μ-oxide) types can be synthesised. We are working towards such aims.

Acknowledgements

We would like to thank our co-workers on the dca and tcm work, Dr. Boujemaa Moubaraki, Dr. Paul Jensen, Anna Kutasi, Patricia van der Werff, David Price, Alexander Harris, Angela Ziebell, Emily Tan, Dr. Gary Fallon, Dr. David Hockless, Professor Richard Robson, the late Dr. Bernard Hoskins, Dr. Brendan Abrahams, Dr. Cameron Kepert and Dr. Mohamedally Kurmoo. This work was funded by grants from the Australian Research Council and the Monash Research Fund, and we would also like to thank Degussa AG for their generous donation of Na(dca).

References

[1] R. Robson, B.F. Hoskins, J. Am. Chem. Soc. 112 (1990) 1546.
[2] (a) S.R. Batten, K.S. Murray, Aust. J. Chem. 54 (2001) 605;
(b) S. Kitagawa, M. Kondo, Bull. Chem. Soc. Jpn. 5 (2001) 107;
(c) K.A. Hirsch, S.C. Wilson, J.S. Moore, Chem. Eur. J. 3 (1997) 765;
(d) M.J. Zaworotko, Chem. Soc. Rev. 23 (1994) 283;
(e) L. Carlucci, G. Ciani, D.M. Proserpio, F. Porta, Angew. Chem. Int. Ed. 42 (2003) 317;
(f) D.M.L. Goodgame, S. Menzer, A.M. Smith, D.J. Williams, J. Chem. Soc. Dalton Trans. (1997) 3213;

(g) A.J. Blake, N.R. Champness, P. Hubberstey, W.-S. Li, M.A. Withersby, M. Schroder, Coord. Chem. Rev. 183 (1999) 117;
(h) M. Munakata, L.P. Wu, T. Kuroda-Sowa, Bull. Chem. Soc. Jpn. 70 (1997) 1727;
(i) R. Robson, J. Chem. Soc. Dalton Trans. (2000) 3735;
(j) M. Munakata, L.P. Wu, T. Kuroda-Sowa, Adv. Inorg. Chem. 46 (1998) 173;
(k) P.J. Hagrman, D. Hagrman, J. Zubieta, Angew. Chem. Int. Ed. 38 (1999) 2638;
(l) C.J. Kepert, M.J. Rosseinsky, Chem. Commun. (1998) 31;
(m) J. Tao, Y. Zhang, M.-L. Tong, X.-M. Chen, T. Yuen, C.L. Lin, X. Huang, J. Li, Chem. Commun. (2002) 1342;
(n) S.W. Keller, S. Lopez, J. Am. Chem. Soc. (1999) 6306;
(o) J.Y. Lu, E.E. Kohler, Inorg. Chem. Commun. 5 (2002) 600;
(p) Y. Diskin-Posner, S. Dahal, I. Goldberg, Angew. Chem. Int. Ed. 39 (2000) 1288;
(q) C.V.K. Sharma, Cryst. Growth Des. 2 (2002) 465;
(r) A. Jouaiti, M.W. Hosseini, N. Kyritsakas, Chem. Commun. (2002) 1898;
(s) J.D. Ranford, J.J. Vittal, D. Wu, X. Yang, Angew. Chem. Int. Ed. 38 (1999) 3498;
(t) V.V. Ponomarova, V.V. Komarchuk, I. Boldog, A.N. Chernega, J. Sieler, K.V. Domasevitch, Chem. Commun. (2002) 436;
(u) P.L. Caradoc-Davies, L.R. Hanton, Chem. Commun. (2001) 1098;
(v) Z. Xu, Y.-H. Kiang, S. Lee, E.B. Lobkovsky, N. Emmott, J. Am. Chem. Soc. 122 (2000) 8376;
(w) X. Xue, X.-S. Wang, L.-Z. Wang, R.-G. Xiong, B.F. Abrahams, X.-Z. You, Z.-L. Xue, C.-M. Che, Inorg. Chem. 41 (2002) 6544;
(x) M. Du, X.-H. Bu, Y.-M. Guo, H. Liu, S.R. Batten, J. Ribas, T.C.W. Mak, Inorg. Chem. 41 (2002) 4904;
(y) G.S. Papaefstathiou, L.R. MacGillivray, Angew. Chem. Int. Ed. 41 (2002) 2070;
(z) B. Moulton, M.J. Zaworotko, Chem. Rev. 101 (2001) 1629.

[3] (a) S.R. Batten, R. Robson, Angew. Chem. Int. Ed. 37 (1998) 1460;
(b) S.R. Batten, Cryst. Eng. Commun. 3 (2001) 67.

[4] S.R. Batten, Curr. Opin. Solid State Mater. Sci. 5 (2001) 107.

[5] (a) M. Kondo, T. Okubo, A. Asami, S. Noro, T. Yoshitomi, S. Kitagawa, T. Ishii, H. Matsuzaka, K. Seki, Angew. Chem. Int. Ed. 38 (1999) 140;
(b) M. Kondo, M. Shimamura, S. Noro, S. Minakoshi, A. Asami, K. Seki, S. Kitagawa, Chem. Mater. 12 (2000) 1288;
(c) R. Kitaura, K. Seki, G. Akiyama, S. Kitagawa, Angew. Chem. Int. Ed. 42 (2003) 428;
(d) R. Kitaura, K. Fujimoto, S. Noro, M. Kondo, S. Kitagawa, Angew. Chem. Int. Ed. 41 (2002) 133;
(e) S. Noro, S. Kitagawa, M. Kondo, K. Seki, Angew. Chem. Int. Ed. 39 (2000) 2081;
(f) O.M. Yaghi, H. Li, C. Davis, D. Richardson, T.L. Groy, Acc. Chem. Res. 31 (1998) 474;
(g) M. Eddaoudi, D.B. Moler, H. Li, B. Chen, T.M. Reineke, M. O'Keeffe, O.M. Yaghi, Acc. Chem. Res. 34 (2001) 319;
(h) N.L. Rosi, M. Eddaoudi, J. Kim, M. O'Keeffe, O.M. Yaghi, Cryst. Eng. Commun. 4 (2002) 401;
(i) M. Eddaoudi, J. Kim, N. Rosi, D. Vodak, J. Wachter, M. O'Keeffe, O.M. Yaghi, Science 295 (2002) 469;
(j) H. Li, M. Eddaoudi, M. O'Keeffe, O.M. Yaghi, Nature 402 (1999) 276;
(k) A.J. Fletcher, E.J. Cussen, T.J. Prior, M.J. Rosseinsky, C.J. Kepert, K.M. Thomas, J. Am. Chem. Soc. 123 (2001) 10001;
(l) C.J. Kepert, T.J. Prior, M.J. Rosseinsky, J. Am. Chem. Soc. 122 (2000) 5158;
(m) E.J. Cussen, J.B. Claridge, M.J. Rosseinsky, C.J. Kepert, J. Am. Chem. Soc. 124 (2002) 9574;
(n) B.F. Abrahams, P.A. Jackson, R. Robson, Angew. Chem. Int. Ed. 37 (1998) 2656.

[6] (a) M. Fujita, Y.J. Kwon, S. Washizu, K. Ogura, J. Am. Chem. Soc. 116 (1994) 1151;
(b) J.S. Seo, D. Whang, H. Lee, S.I. Jun, J. Oh, Y.J. Jeon, K. Kim, Nature 404 (2000) 982.

[7] (a) O.R. Evans, W. Lin, Chem. Mater. 13 (2001) 2705;
(b) O.R. Evans, W. Lin, Chem. Mater. 13 (2001) 3009.

[8] (a) G.J. Halder, C.J. Kepert, B. Moubaraki, K.S. Murray, J.D. Cashion, Science 298 (2002) 1762;
(b) L.G. Beauvais, M.P. Shores, J.R. Long, J. Am. Chem. Soc. 122 (2000) 2763.

[9] (a) J.A. Real, A.B. Gaspar, V. Niel, M.C. Munoz, Coord. Chem. Rev. 236 (2003) 121;
(b) V. Niel, M.C. Munoz, A.B. Gaspar, A. Galet, G. Levchenko, J.A. Real, Chem. Eur. J. 8 (2002) 2446;
(c) N. Moliner, C. Munoz, S. Letard, X. Solans, N. Menendez, A. Goujon, F. Varret, J.A. Real, Inorg. Chem. 39 (2000) 5390;
(d) O. Kahn, C.J. Martinez, Science 279 (1998) 44.

[10] O. Kahn, Adv. Inorg. Chem. 43 (1995) 179.

[11] (a) C. Mathoniere, C.J. Nuttall, S.G. Carling, P. Day, Inorg. Chem. 35 (1996) 1201;
(b) S. Decurtins, R. Pellaux, G. Antorrena, F. Palacio, Coord. Chem. Rev. 190-192 (1999) 841.

[12] (a) M. Ohba, H. Okawa, Coord. Chem. Rev. 198 (2000) 313;
(b) M. Verdaguer, A. Bleuzen, C. Train, R. Garde, F. Fabrizi de Biani, C. Desplanches, in: P. Day A.E. Underhill (Eds.), Metal-organic and Organic Molecular Magnets, Royal Society of Chemistry, Cambridge, 2000, p. 105;
(c) K. Hashimoto, S. Ohkoshi, in: P. Day A.E. Underhill (Eds.), Metal-organic and Organic Molecular Magnets, Royal Society of Chemistry, Cambridge, 2000, p. 123;
(d) K. Dunbar, R. Heintze, Prog. Inorg. Chem. 45 (1997) 283.

[13] (a) A. Escuer, R. Vicente, M.A.S. Goher, F.A. Mautner, Inorg. Chem. 37 (1998) 782;
(b) J. Ribas, A. Escuer, M. Monfort, R. Vicente, R. Cortes, L. Lezama, T. Rojo, Coord. Chem. Rev. 193-195 (1999) 1027;
(c) J.L. Manson, A.M. Arif, J.S. Miller, Chem. Commun. (1999) 1479;
(d) L. Shen, Y.-Z. Xu, J. Chem. Soc. Dalton Trans. (2001) 3413.

[14] S.R. Batten, P. Jensen, B. Moubaraki, K.S. Murray, R. Robson, Chem. Commun. (1998) 439.

[15] M. Kurmoo, C.J. Kepert, New J. Chem. 22 (1998) 1515.

[16] J.L. Manson, C.R. Kmety, Q.-Z. Huang, J.W. Lynn, G.M. Bendele, S. Pagola, P.W. Stephens, L.M. Liable-Sands, A.L. Rheingold, A.J. Epstein, J.S. Miller, Chem. Mater. 10 (1998) 2552.

[17] (a) J. Cho, U. Lee, J.C. Kim, Transition Met. Chem. 27 (2002) 429;
(b) Z.-M. Wang, J. Luo, B.-W. Sun, C.-H. Yan, C.-S. Liao, S. Gao, Acta Crystallogr. Sect. C 56 (2000) e242;
(c) I. Potocnak, M. Dunaj-Jurco, D. Miklos, W. Massa, L. Jager, Acta Crystallogr. Sect. C 57 (2001) 363;
(d) K.E. Bessler, L.L. Romualdo, P.d.T.S. Filho, V.M. Deflon, C. Maichle-Mossmer, Z. Anorg. Allg. Chem. 627 (2001) 651;
(e) J. Luo, M. Hong, Y. Liang, R. Cao, Acta Crystallogr. Sect. E 57 (2001) m529;
(f) R. Clerac, F.A. Cotton, S.P. Jeffery, C.A. Murillo, X. Wang, Inorg. Chem. 40 (2001) 1265;
(g) S.-M. Kuang, P.E. Fanwick, R.A. Walton, Inorg. Chem. 40 (2001) 5682;
(h) W. Sacher, U. Nagel, W. Beck, Chem. Ber. 120 (1987) 895;
(i) A. Maslejova, I. Potocnak, J. Sima, M. Kabesova, J. Coord. Chem. 43 (1998) 41;
(j) J.-C. Wang, Y. Wang, Acta Crystallogr. Sect. C 49 (1993) 131;
(k) D.A. Summerville, I.A. Cohen, K. Hatano, W.R. Scheidt, Inorg. Chem. 17 (1978) 2906;
(l) T.J. Johnson, M.R. Bond, R.D. Willett, Acta Crystallogr. Sect. C 44 (1988) 1890;
(m) S.L. Schiavo, G. Bruno, P. Zanello, F. Laschi, P. Piraino, Inorg. Chem. 36 (1997) 1004;

(n) I. Potocnak, M. Dunaj-Jurco, D. Miklos, L. Jager, Acta Crystallogr. Sect. C 53 (1997) 1215;
(o) J.-C. Wang, L.J. Shih, Y.-J. Chen, Y. Wang, F.R. Fronczek, S.F. Watkins, Acta Crystallogr. Sect. B 49 (1993) 680;
(p) A. Nedelcu, Z. Zak, A.M. Madalan, J. Pinkas, M. Andruh, Polyhedron 22 (2003) 789;
(q) I. Potocnak, M. Dunaj-Jurco, D. Miklos, M. Kabesova, L. Jager, Acta Crystallogr. Sect. B 51 (1995) 600;
(r) I. Potocnak, M. Dunaj-Jurco, D. Miklos, L. Jager, Monatsh. Chem. 132 (2001) 315;
(s) I. Potocnak, M. Dunaj-Jurco, D. Miklos, L. Jager, Acta Crystallogr. Sect. C 52 (1996) 1653;
(t) M. Dunaj-Jurco, D. Miklos, I. Potocnak, L. Jager, Acta Crystallogr. Sect. C 52 (1996) 2409;
(u) J. Kozisek, H. Paulus, M. Dankova, M. Hvastijova, Acta Crystallogr. Sect. C 52 (1996) 3019.

[18] (a) I. Potocnak, M. Burcak, W. Massa, L. Jager, Acta Crystallogr. Sect. C 58 (2002) m523;
(b) F. Brezina, Z. Travnicek, Z. Sindelar, R. Pastorek, J. Marek, Transition Met. Chem. 24 (1999) 459;
(c) L.-Y. Zhang, L.-X. Shi, Z.-N. Chen, Inorg. Chem. 42 (2003) 633.

[19] (a) B.Z. Narymbetov, E. Canadell, T. Togonidze, S.S. Khasanov, L.V. Zorina, R.P. Shibaeva, H. Kobayashi, J. Mater. Chem. 11 (2001) 332;
(b) Y. He, H.-Z. Kou, B.C. Zhou, M. Xiong, R.-J. Wang, Y. Li, Acta Crystallogr. Sect. E 58 (2002) m389;
(c) I. Potocnak, M. Pohlova, C. Wagner, L. Jager, Acta Crystallogr. Sect. E 58 (2002) m595;
(d) B. Jurgens, H.A. Hoppe, E. Irran, W. Schnick, Inorg. Chem. 41 (2002) 4849;
(e) S. Triki, F. Thetiot, J.S. Pala, S. Golhen, J.M. Clemente-Juan, C.J. Gomez-Garcia, E. Coronado, Chem. Commun. (2001) 2172;
(f) J.-C. Wang, L.-Y. Chou, W.-Y. Hsien, Acta Crystallogr. Sect. C 50 (1994) 879;
(g) V.V. Skopenko, A.A. Kapshuk, Koord. Khim. 11 (1985) 1202;
(h) M.A. Beno, H.H. Wang, L. Soderholm, K.D. Carlson, L.N. Hall, L. Nunez, H. Rummens, B. Anderson, J.A. Schlueter, J.M. Williams, M.-H. Whangbo, M. Evain, Inorg. Chem. 28 (1989) 150;
(i) D.A. Dixon, J.C. Calabrese, J.S. Miller, J. Am. Chem. Soc. 108 (1986) 2582;
(j) T.V. Baukova, D.N. Kravtsov, L.G. Kuzmina, N.V. Dvortsova, M.A. Poray-Koshits, E.G. Perevalova, J. Organomet. Chem. 372 (1989) 465;
(k) I. Potocnak, M. Dunaj-Jurco, D. Miklos, L. Jager, Acta Crystallogr. Sect. C 54 (1998) 313;
(l) I. Potocnak, M. Dunaj-Jurco, D. Miklos, L. Jager, Acta Crystallogr. Sect. C 52 (1996) 48;
(m) R. Desiderato, R.L. Sass, Acta Crystallogr. 18 (1965) 1;
(n) J.K. Kochi, C.H. Wei, J. Organomet. Chem. 451 (1993) 111;
(o) I. Potocnak, M. Dunaj-Jurco, D. Miklos, L. Jager, Acta Crystallogr. Sect. C 54 (1998) 1760;
(p) C. Bugg, R. Desiderato, R.L. Sass, J. Am. Chem. Soc. 86 (1964) 3157;
(q) I. Potocnak, M. Dunaj-Jurco, D. Miklos, L. Jager, Acta Crystallogr. Sect. C 52 (1996) 532.

[20] (a) M. Gembicky, R. Boca, L. Jager, C. Wagner, Inorg. Chem. Commun. 3 (2000) 566;
(b) K.E. Bessler, L.A. de, P. Calzavara, V.M. Deflon, E. Niquet, Acta Crystallogr. Sect. E 57 (2001) m522;
(c) S.-M. Kuang, P.E. Fanwick, R.A. Walton, Inorg. Chem. 41 (2002) 147.

[21] H. Köhler, in: A.M. Golub H. Köhler V.V. Skopenko (Eds.), Chemistry of Pseudohalides, Elsevier, Amsterdam, 1987 (chapters 7 and 8).

[22] J. Kohout, L. Jager, M. Hvastijova, J. Kozisek, J. Coord. Chem. 51 (2000) 169.

[23] J.S. Miller, J.L. Manson, Acc. Chem. Res. 34 (2001) 563.

[24] V.I. Ovcharenko, R.Z. Sagdeev, Russ. Chem. Rev. 68 (1999) 345.

[25] (a) W.H. Baddley, Inorg. Chim. Acta Rev. 2 (1968) 7;
(b) W. Beck, W.P. Fehlhammer, in: C.C. Addison, D.B. Sowerby (Eds.), MTP Int. Rev. Sci.: Inorg. Chem., Ser. One, Medical and Technical Publishing Co., Oxford, 2 (1972) 253.

[26] P. Jensen, S.R. Batten, G.D. Fallon, B. Moubaraki, K.S. Murray, D.J. Price, Chem. Commun. (1999) 177.

[27] S.R. Batten, P. Jensen, C.J. Kepert, M. Kurmoo, B. Moubaraki, K.S. Murray, D.J. Price, J. Chem. Soc. Dalton Trans. (1999) 2987.

[28] C.R. Kmety, J.L. Manson, Q. Huang, J.W. Lynn, R.W. Erwin, J.S. Miller, A.J. Epstein, Phys. Rev. B 60 (1999) 60.

[29] C.R. Kmety, Q. Huang, J.W. Lynn, R.W. Erwin, J.L. Manson, S. McCall, J.E. Crow, K.L. Stevenson, J.S. Miller, A.J. Epstein, Phys. Rev. B 62 (2000) 5576.

[30] T. Jestadt, M. Kurmoo, S.J. Blundell, F.L. Pratt, C.J. Kepert, K. Prassides, B.W. Lovett, I.M. Marshall, A. Husmann, K.H. Chow, R.M. Valladares, C.M. Brown, A. Lappas, J. Phys.: Condens. Matter 13 (2001) 2263.

[31] S.J. Blundell, J.S. Miller M. Drillon (Eds.), Magnetism: Molecules and Materials, Wiley VCH, Weinheim, 2001, p. 235.

[32] S.R. Batten, J.D. Cashion, B. Moubaraki, K.S. Murray, D.J. Price, unpublished results.

[33] See also (a) K.S. Murray, S.R. Batten, B. Moubaraki, D.J. Price, R. Robson, Mol. Cryst. Liq. Cryst. 335 (1999) 313; (b) C.R. Kmety, J.L. Manson, Q.-Z. Huang, J.W. Lynn, R.W. Erwin, J.S. Miller, A.J. Epstein, Mol. Cryst. Liq. Cryst. 334 (1999) 631; (c) M. Kurmoo, C.J. Kepert, Mol. Cryst. Liq. Cryst. 334 (1999) 693; (d) M.R. Pederson, A.Y. Liu, T. Baruah, E.Z. Kurmaev, A. Moewes, S. Chiuzbaian, M. Neumann, C.R. Kmety, K.L. Stevenson, D. Ederer, Phys. Rev. B 66 (2002) 014446; (e) S.J. Blundell, A. Husmann, T. Jestadt, F.L. Pratt, I.M. Marshall, B.W. Lovett, M. Kurmoo, T. Sugano, W. Hayes, Physica B 289-290 (2000) 115.

[34] C.J. Nuttall, T. Takenobu, Y. Iwasa, M. Kurmoo, Mol. Cryst. Liq. Cryst. 342 (2000) 227.

[35] A. Lappas, A.S. Wills, M.A. Green, K. Prassides, M. Kurmoo, Phys. Rev. B 67 (2003) 144406.

[36] J.L. Manson, C.R. Kmety, F. Palacio, A.J. Epstein, J.S. Miller, Chem. Mater. 13 (2001) 1068.

[37] H.N. Bordallo, J.L. Manson, L. Chapon, R. Feyerherm, J.R.D. Copley, Abstracts of VIIIth International Conference on Molecule-based Magnets, Valencia, Spain, (2002) A-21.

[38] J.L. Manson, C.R. Kmety, A.J. Epstein, J.S. Miller, Inorg. Chem. 38 (1999) 2552.

[39] C.R. Kmety, J.L. Manson, S. McCall, J.E. Crow, K.L. Stevenson, A.J. Epstein, J. Mag. Mag. Mater. 248 (2002) 52.

[40] J.B. Goodenough, Magnetism and the Chemical Bond, Wiley, New York, 1963.

[41] P.W. Anderson, Phys. Rev. 79 (1950) 705.

[42] J. Kanamori, J. Phys. Chem. Solids 10 (1959) 87.

[43] J.S. Miller, Polyhedron 20 (2001) 1723.

[44] E. Ruiz, C. Desplanches, A. Rodriguez-Fortea, S. Alvarez, Abstracts of VIIIth International Conference on Molecule-based Magnets, Valencia, Spain, (2002) F-7.

[45] (a) S.R. Batten, B.F. Hoskins, R. Robson, J. Chem. Soc. Chem. Commun. (1991) 445;
(b) C. Biondi, M. Bonamico, L. Torelli, A. Vaciago, Chem. Commun. (1965) 191.

[46] S.R. Batten, B.F. Hoskins, B. Moubaraki, K.S. Murray, R. Robson, J. Chem. Soc. Dalton Trans. (1999) 2977.

[47] J.L. Manson, C. Campana, J.S. Miller, Chem. Commun. (1998) 251.

[48] H. Hoshino, K. Iida, T. Kawamoto, T. Mori, Inorg. Chem. 38 (1999) 4229.

[49] J.L. Manson, E. Ressouche, J.S. Miller, Inorg. Chem. 39 (2000) 1135.

[50] R. Feyerherm, A. Loose, J.L. Manson, J. Phys.: Condens. Matter 15 (2003) 663.
[51] P. Jensen, D.J. Price, S.R. Batten, B. Moubaraki, K.S. Murray, Chem. Eur. J. 6 (2000) 3186.
[52] J.L. Manson, D.W. Lee, A.L. Rheingold, J.S. Miller, Inorg. Chem. 37 (1998) 5966.
[53] (a) Y.-J. Shi, X.-T. Chen, Y.-Z. Li, Z. Xue, X.-Z. You, New J. Chem. 26 (2002) 1711;
(b) B. Jurgens, H.A. Hoppe, W. Schnick, Solid State Sci. 4 (2002) 821.
[54] D. Britton, Y.M. Chow, Acta Crystallogr. Sect. B 33 (1977) 697.
[55] D. Britton, Acta Crystallogr. Sect. C 46 (1990) 2297.
[56] J. Konnert, D. Britton, Inorg. Chem. 5 (1966) 1193.
[57] S.R. Batten, B.F. Hoskins, R. Robson, New J. Chem. 22 (1998) 173.
[58] B.F. Abrahams, S.R. Batten, B.F. Hoskins, R. Robson, Inorg. Chem. 42 (2003) 2654.
[59] K. Brodersen, J. Hofmann, Z. Anorg. Allg. Chem. 609 (1992) 29.
[60] B. Jurgens, E. Irran, W. Schnick, J. Solid State Chem. 157 (2001) 241.
[61] (a) P. Starynowicz, Acta Crystallogr. Sect. C 47 (1991) 2198;
(b) B. Jurgens, W. Milius, P. Morys, W. Schnick, Z. Anorg. Allg. Chem. 624 (1998) 91;
(c) B. Jurgens, E. Irran, J. Schneider, W. Schnick, Inorg. Chem. 39 (2000) 665;
(d) E. Irran, B. Jurgens, W. Schnick, Chem. Eur. J. 7 (2001) 5372.
[62] (a) P. Andersen, B. Klewe, E. Thom, Acta Chem. Scand. 21 (1967) 1530;
(b) P. Andersen, B. Klewe, Nature 200 (1963) 464;
(c) J.R. Witt, D. Britton, Acta Crystallogr. Sect. B 27 (1971) 1835.
[63] J.-P. Renard, L.-P. Regnault, M. Verdaguer, in: J.S. Miller M. Drillon (Eds.), Magnetism: Molecules and Materials, Wiley VCH, Weinheim, 2001, p. 49.
[64] A. Caneschi, D. Gatteschi, N. Lalioti, C. Sangregorio, R. Sessoli, G. Venturi, A. Vindigni, A. Rettori, M.G. Pini, M.A. Novak, Angew. Chem. Int. Ed. 40 (2001) 1760.
[65] S.R. Marshall, C.D. Incarvito, J.L. Manson, A.L. Rheingold, J.S. Miller, Inorg. Chem. 39 (2000) 1969.
[66] (a) M.E. Fisher, Am. J. Phys. 32 (1964) 343;
(b) R. Georges, J.J. Borras-Almenar, E. Coronado, J. Curely, M. Drillon, in: J.S. Miller M. Drillon (Eds.), Magnetism: Molecules and Materials, Wiley VCH, Weinheim, 2001, p. 1;
(c) O. Kahn, Molecular Magnetism, VCH, New York, 1993, p. 258.
[67] S. Martin, M.G. Barandika, J.I.R. de Larramendi, R. Cortes, M. Font-Bardia, L. Lezama, Z.E. Serna, X. Solans, T. Rojo, Inorg. Chem. 40 (2001) 3687.
[68] S. Kitagawa, T. Okubo, S. Kawata, M. Kondo, M. Katada, H. Kobayashi, Inorg. Chem. 34 (1995) 4790.
[69] J. Kozisek, M. Hvastijova, J. Kohout, J. Mrozinski, H. Kohler, J. Chem. Soc. Dalton Trans. (1991) 1773.
[70] B. Vangdal, J. Carranza, F. Lloret, M. Julve, J. Sletten, J. Chem. Soc. Dalton Trans. (2002) 566.
[71] I. Potocnak, M. Burcak, C. Wagner, L. Jager, Acta Crystallogr. Sect. C 58 (2002) m327.
[72] J. Carranza, C. Brennan, J. Sletten, F. Lloret, M. Julve, J. Chem. Soc. Dalton Trans. (2002) 3164.
[73] J.W. Hall, Ph.D. Dissertation, University of North Carolina, Chapel Hill, NC (1977).
[74] A. Escuer, F.A. Mautner, N. Sanz, R. Vincente, Inorg. Chim. Acta 340 (2002) 163.
[75] D.J. Price, S.R. Batten, B. Moubaraki, K.S. Murray, Indian J. Chem., in press.
[76] A. Claramunt, A. Escuer, F.A. Mautner, N. Sanz, R. Vicente, J. Chem. Soc. Dalton Trans. (2000) 2627.
[77] Q. Shi, R. Cao, X. Li, J. Luo, M. Hong, Z. Chen, New J. Chem. 26 (2002) 1397.
[78] B.J. Kennedy, K.S. Murray, Inorg. Chem. 24 (1985) 1552.
[79] S. Sailaja, K.R. Reddy, M.V. Rajasekharan, C. Hureau, E. Riviere, J. Cano, J.J. Girerd, Inorg. Chem. 42 (2003) 180.
[80] D.A. Summerville, I.A. Cohen, K. Hatano, W.R. Scheidt, Inorg. Chem. 17 (1978) 2906.
[81] B. Latte, L. Galich, H. Homborg, B. Moubaraki, K.S. Murray, in preparation.
[82] B.J. Kennedy, K.S. Murray, Inorg. Chem. 24 (1985) 1557.
[83] D.K. Rittenberg, J.S. Miller, Inorg. Chem. 38 (1999) 4838.
[84] A.P. Purdy, E. Houser, C.F. George, Polyhedron 16 (1997) 3671.
[85] K.E. Bessler, L.L. Romualdo, V.M. Deflon, A. Hagenbach, Z. Anorg. Allg. Chem. 626 (2000) 1942.
[86] B. Li, J. Ding, J. Lang, Z. Xu, J. Chen, J. Mol. Struct. 616 (2002) 175.
[87] H. Miyasaka, R. Clerac, C.S. Campos-Fernandez, K.R. Dunbar, Inorg. Chem. 40 (2001) 1663.
[88] J.L. Manson, A.M. Arif, C.D. Incarvito, L.M. Liable-Sands, A.L. Rheingold, J.S. Miller, J. Solid State Chem. 145 (1999) 369.
[89] A. Escuer, F.A. Mautner, M. Sanz, R. Vicente, Inorg. Chem. 39 (2000) 1668.
[90] B.-W. Sun, S. Gao, B.-Q. Ma, Z.-M. Wang, Inorg. Chem. Commun. 4 (2001) 72.
[91] J. Luo, M. Hong, J. Weng, Y. Zhao, R. Cao, Inorg. Chim. Acta 329 (2002) 59.
[92] G.A. van Albada, I. Mutikainen, U. Turpeinen, J. Reedijk, Acta Crystallogr. Sect. E 57 (2001) m421.
[93] J.L. Manson, A.M. Arif, J.S. Miller, J. Mater. Chem. 9 (1999) 979.
[94] G.A. van Albada, M.E. Quiroz-Castro, I. Mutikainen, U. Turpeinen, J. Reedijk, Inorg. Chim. Acta 298 (2000) 221.
[95] P. Jensen, Ph.D. thesis, Monash University (2002).
[96] A.M. Kutasi, S.R. Batten, A.R. Harris, B. Moubaraki, K.S. Murray, Aust. J. Chem. 55 (2002) 311.
[97] S.R. Batten, B.F. Hoskins, B. Moubaraki, K.S. Murray, R. Robson, Cryst. Eng. Commun. 3 (2001) 33.
[98] J.L. Manson, C.D. Incarvito, A.M. Arif, A.L. Rheingold, J.S. Miller, Mol. Cryst. Liq. Cryst. 334 (1999) 605.
[99] J.-H. Luo, M.-C. Hong, R. Cao, Y.-C. Liang, Y.-J. Zhao, R.-H. Wang, J.-B. Weng, Polyhedron 21 (2002) 893.
[100] J.L. Manson, J.A. Schlueter, U. Geiser, M.B. Stone, D.H. Reich, Polyhedron 20 (2001) 1423.
[101] P. Jensen, S.R. Batten, B. Moubaraki, K.S. Murray, Chem. Commun. (2000) 793.
[102] P.E. Kruger, G.D. Fallon, B. Moubaraki, K.J. Berry, K.S. Murray, Inorg. Chem. 34 (1995) 4808.
[103] M. Kurmoo, unpublished results.
[104] T. Kusaka, T. Ishida, D. Hashizume, F. Iwasaki, T. Nogami, Chem. Lett. (2000) 1146.
[105] T. Kusaka, T. Ishida, D. Hashizume, F. Iwasaki, T. Nogami, Mol. Cryst. Liq. Cryst. 376 (2002) 463.
[106] P. Jensen, S.R. Batten, B. Moubaraki, K.S. Murray, J. Chem. Soc. Dalton Trans. (2002) 3712.
[107] S. Martin, M.G. Barandika, J.M. Ezpeleta, R. Cortes, J.I.R. de Larramendi, L. Lezama, T. Rojo, J. Chem. Soc. Dalton Trans. (2002) 4275.
[108] S. Dalai, P.S. Mukherjee, E. Zangrando, N.R. Chaudhuri, New J. Chem. 26 (2002) 1185.
[109] J. Curely, Physica B 254 (1998) 277.
[110] M.E. Lines, J. Phys. Chem. Solids 31 (1970) 101.
[111] H. Kooijman, A.L. Spek, G.A. van Albada, J. Reedijk, Acta Crystallogr. Sect. C 58 (2002) m124.
[112] Y.M. Chow, Inorg. Chem. 10 (1971) 1938.
[113] D. Britton, Y.M. Chow, Acta Crystallogr. Sect. C 39 (1983) 1539.
[114] Z.-M. Wang, B.-W. Sun, J. Luo, S. Gao, C.-S. Liao, C.-H. Yan, Y. Li, Inorg. Chim. Acta 332 (2002) 127.
[115] M. Hvastijova, J. Kozisek, J. Kohout, L. Jager, H. Fuess, Transition Met. Chem. 20 (1995) 276.
[116] M. Hvastijova, J. Kohout, J. Kozisek, J.G. Diaz, L. Jager, M. Mrozinski, Z. Anorg. Allg. Chem. 624 (1998) 349.

[117] S.R. Batten, A.R. Harris, P. Jensen, K.S. Murray, A. Ziebell, J. Chem. Soc. Dalton Trans. (2000) 3829.
[118] Z.-M. Wang, J. Luo, B.-W. Sun, C.-H. Yan, S. Gao, C.-S. Liao, Acta Crystallogr. Sect. C 56 (2000) 786.
[119] I. Dasna, S. Golhen, L. Ouahab, O. Pena, J. Guillevic, M. Fettouhi, J. Chem. Soc. Dalton Trans. (2000) 129.
[120] I. Dasna, S. Golhen, L. Ouahab, M. Fettouhi, O. Pena, N. Daro, J.-P. Sutter, Inorg. Chim. Acta 326 (2001) 37.
[121] I. Dasna, S. Golhen, L. Ouahab, O. Pena, N. Daro, J.-P. Sutter, C. R. Acad. Sci. Paris Chimie 4 (2001) 125.
[122] I. Dasna, S. Golhen, L. Ouahab, N. Daro, J.-P. Sutter, New J. Chem. 25 (2001) 1572.
[123] A.M. Kutasi, S.R. Batten, B. Moubaraki, K.S. Murray, J. Chem. Soc. Dalton Trans. (2002) 819.
[124] E. Coronado, C.J. Gomez-Garcia, A. Nuez, F.M. Romero, E. Rusanov, H. Stoeckli-Evans, Inorg. Chem. 41 (2002) 4615.
[125] A.M. Kutasi, S.R. Batten, B. Moubaraki, K.S. Murray, unpublished results.
[126] M. Kurmoo, Chem. Mater. 11 (1999) 3370.
[127] M. Kurmoo, Mol. Cryst. Liq. Cryst. 342 (2000) 167.
[128] Y.M. Chow, D. Britton, Acta Crystallogr. Sect. B 31 (1975) 1934.
[129] M. Hvastijova, J. Kohout, M. Okruhlica, J. Mrozinski, L. Jager, Transition Met. Chem. 18 (1993) 579.
[130] J. Mrozinski, M. Hvastijova, J. Kohout, Polyhedron 11 (1992) 2867.
[131] V. Jacob, S. Mann, G. Huttner, O. Walter, L. Zsolnai, E. Kaifer, P. Rutsch, P. Kircher, E. Bill, Eur. J. Inorg. Chem. (2001) 2625.
[132] S.R. Marshall, C.D. Incarvito, W.W. Shum, A.L. Rheingold, J.S. Miller, Chem. Commun. (2002) 3006.
[133] N. Moliner, A.B. Gaspar, M.C. Munoz, V. Niel, J. Cano, J.A. Real, Inorg. Chem. 40 (2001) 3986.
[134] J.P. Smith, B.A. Leita, B. Moubaraki, K.S. Murray, unpublished results.
[135] N. Ortega-Villar, R. Moreno-Esparza, V. Niel, A. Gaspar, M.C. Munoz, J.A. Real, Abstracts of VIIIth International Conference on Molecule-based Magnets, Valencia, Spain, (2002) C-33.
[136] P. Jensen, S.R. Batten, G.D. Fallon, D.C.R. Hockless, B. Moubaraki, K.S. Murray, R. Robson, J. Solid State Chem. 145 (1999) 387.
[137] P. Jensen, S.R. Batten, B. Moubaraki, K.S. Murray, J. Solid State Chem. 159 (2001) 352.
[138] J.L. Manson, C.D. Incarvito, A.L. Rheingold, J.S. Miller, J. Chem. Soc. Dalton Trans. (1998) 3705.
[139] J.L. Manson, Q.-Z. Huang, J.W. Lynn, H.-J. Koo, M.-H. Whangbo, R. Bateman, T. Otsuka, N. Wada, D.N. Argyriou, J.S. Miller, J. Am. Chem. Soc. 123 (2001) 162.
[140] C.M. Brown, J.L. Manson, J. Am. Chem. Soc. 124 (2002) 12600.
[141] G.S. Rushbrooke, P.J. Wood, Mol. Phys. 1 (1958) 257.
[142] S. Triki, F. Thetiot, J.-R. Galan-Mascaros, J.S. Pala, K.R. Dunbar, New J. Chem. 25 (2001) 954.
[143] W.-F. Yeung, S. Gao, W.-T. Wong, T.-C. Lau, New J. Chem. 26 (2002) 523.
[144] I. Riggio, G.A. van Albada, D.D. Ellis, A.L. Spek, J. Reedijk, Inorg. Chim. Acta 313 (2001) 120.
[145] B.-W. Sun, S. Gao, B.-Q. Ma, Z.-M. Wang, New J. Chem. 24 (2000) 953.
[146] B.-W. Sun, S. Gao, Z.-M. Wang, Chem. Lett. (2001) 2.
[147] M.A. Lawandy, X. Huang, R.-J. Wang, J. Li, J.Y. Lu, T. Yueh, C.L. Lin, Inorg. Chem. 38 (1999) 5410.
[148] S. Han, J.L. Manson, J. Kim, J.S. Miller, Inorg. Chem. 39 (2000) 4182.
[149] E.-Q. Gao, Z.-M. Wang, C.-S. Liao, C.-H. Yan, New J. Chem. 26 (2002) 1096.
[150] S.R. Batten, B.F. Hoskins, R. Robson, Chem. Eur. J. 6 (2000) 156.
[151] A.M. Kutasi, S.R. Batten, A.R. Harris, B. Moubaraki, K.S. Murray, Cryst. Eng. Commun. 4 (2002) 202.
[152] B.-W. Sun, S. Gao, B.-Q. Ma, D.-Z. Niu, Z.-M. Wang, J. Chem. Soc. Dalton Trans. (2000) 4187.
[153] S.R. Batten, B.F. Hoskins, R. Robson, Inorg. Chem. 37 (1998) 3432.
[154] S.R. Batten, B.F. Hoskins, R. Robson, Angew. Chem. Int. Ed. Engl. 36 (1997) 636.
[155] S. Martin, M.G. Barandika, R. Cortes, J.I.R. de Larramendi, M.K. Urtiaga, L. Lezama, M.I. Arriortua, T. Rojo, Eur. J. Inorg. Chem. (2001) 2107.
[156] S.R. Marshall, A.L. Rheingold, L.N. Dawe, W.W. Shum, C. Kitamura, J.S. Miller, Inorg. Chem. 41 (2002) 3599.
[157] T. Jestadt, M. Kurmoo, S.J. Blundell, B.W. Lovett, F.L. Pratt, W. Hayes, Synth. Met. 103 (1999) 2325.
[158] A.M. Kutasi, S.R. Batten, A.R. Harris, B. Moubaraki, K.S. Murray, unpublished results.
[159] P.M. van der Werff, S.R. Batten, P. Jensen, B. Moubaraki, K.S. Murray, Inorg. Chem. 40 (2001) 1718.
[160] J.W. Raebiger, J.L. Manson, R.D. Sommer, U. Geiser, A.L. Rheingold, J.S. Miller, Inorg. Chem. 40 (2001) 2578.
[161] M. Scudder, I. Dance, J. Chem. Soc. Dalton Trans. (1998) 3155.
[162] S. Lorenzo, C. Horn, D. Craig, M. Scudder, I. Dance, Inorg. Chem. 39 (2000) 401.
[163] P.M. van der Werff, S.R. Batten, P. Jensen, B. Moubaraki, K.S. Murray, unpublished results.
[164] P.M. van der Werff, S.R. Batten, P. Jensen, B. Moubaraki, K.S. Murray, E.H.-K. Tan, Polyhedron 20 (2001) 1129.
[165] L.J. De Jongh (Eds.), Magnetic Properties of Layered Transition Metal Compounds, Kluwer Academic Publishers, Dordrecht, Boston, MA, 1990.
[166] L. Jager, C. Wagner, M. Korabik, A. Zygmunt, J. Mrozinski, J. Mol. Struct. 570 (2001) 159.
[167] S.R. Batten, P. Jensen, B. Moubaraki, K.S. Murray, Chem. Commun. (2000) 2331.
[168] (a) A.M. Kini, U. Geiser, H.H. Wang, K.D. Carlson, J.M. Williams, W.K. Kwok, K.G. Vandervoort, J.E. Thompson, D.L. Stupka, D. Jung, M.-H. Whangbo, Inorg. Chem. 29 (1990) 2555;
(b) J.M. Williams, A.M. Kini, H.H. Wang, K.D. Carlson, U. Geiser, L.K. Montgomery, G.J. Pyrka, D.M. Watkins, J.M. Kommers, S.J. Boryschuk, A.V.S. Crouch, W.K. Kwok, J.E. Schirber, D.L. Overmyer, D. Jung, M.-H. Whangbo, Inorg. Chem. 29 (1990) 3274;
(c) H.H. Wang, A.M. Kini, L.K. Montgomery, U. Geiser, K.D. Carlson, J.M. Williams, J.E. Thompson, D.M. Watkins, W.K. Kwok, U. Welp, K.G. Vandervoort, Chem. Mater. 2 (1990) 482;
(d) U. Geiser, A.M. Kini, H.H. Wang, M.A. Beno, J.M. Williams, Acta Crystallogr. Sect. C 47 (1991) 190.
[169] T. Komatsu, H. Sato, T. Nakamura, N. Matsukawa, H. Yamochi, G. Saito, M. Kusunoki, K. Sakaguchi, S. Kagoshima, Bull Chem. Soc. Jpn. 68 (1995) 2233.
[170] (a) T. Komatsu, T. Nakamura, N. Matsukawa, H. Yamochi, G. Saito, H. Ito, T. Ishiguro, M. Kusunoki, K. Sakaguchi, Solid State Commun. 80 (1991) 843;
(b) H. Yamochi, T. Nakamura, T. Komatsu, N. Matsukawa, T. Inoue, G. Saito, T. Mori, M. Kusunoki, K. Sakaguchi, Solid State Commun. 82 (1992) 101;
(c) H. Yamochi, T. Komatsu, N. Matsukawa, G. Saito, T. Mori, M. Kusunoki, K. Sakaguchi, J. Am. Chem. Soc. 115 (1993) 11319.
[171] J.A. Manskaya, K.V. Domasevitch, V.R. Polyakov, V.N. Kokozay, O.Y. Vassilieva, Zh. Obschei Khim. 69 (1999) 101.
[172] J.A. Rusanova, P.J. Squattrito, K.V. Domasevitch, V.N. Kokozay, Z. Naturforsch. Teil. B 54b (1999) 389.
[173] P. Day, J. Chem. Soc. Dalton Trans. (1997) 701.
[174] S.J. Rettig, V. Sanchez, A. Storr, R.C. Thompson, J. Trotter Inorg. Chem. 38 (1999) 5920.
[175] A. Altomare, C. Bellitto, S.A. Ibrahim, M.R. Mahmoud, R. Rizzi, J. Chem. Soc. Dalton Trans. (2000) 3913.
[176] P. Day, J. Chem. Soc. Dalton Trans. (2000) 3483.
[177] E. Ruiz, P. Alemany, A. Alvarez, J. Cano, J. Am. Chem. Soc. 118 (1997) 1297.